Allosteric modulation and ligand binding kinetics at the Kv11.1 channel

Yu, Z.

Chapter 7

Structure-affinity relationships (SARs) and structure-kinetics relationships (SKRs) of K_v11.1 (hERG) blockers

Zhiyi Yu
Jacobus P. D. van Veldhoven
Julien Louvel
Ingrid M. E. 't Hart
Martin B. Rook
Marcel A. G. van der Heyden
Laura H. Heitman
Adriaan P. IJzerman

Adapted from J. Med. Chem. ***2015,*** *58, 5916-5929.*

Abstract

We explored structure-kinetics relationships and structure-affinity relationships in four series of K_v11.1 (hERG) blockers. We learned that despite dramatic differences in affinity and association rates, there were hardly any variations in the dissociation rate constants of these molecules with residence times (RTs) of a few minutes only. Hence, we synthesized sixteen novel molecules, in particular in the pyridinium class of compounds, to further address this peculiar phenomenon. We found molecules with very short RTs (< 1 min) and much longer RTs (> 100 min). This enabled us to construct a k_{on}-k_{off}-K_D kinetic map for all compounds, providing a possible framework for a further and more precise categorization of K_v11.1 blockers. Additionally, two representative compounds were tested in patch clamp assays, and their RTs were compared with patch clamp IC_{50} values. Our findings strongly suggest that the simultaneous study of ligand affinity and kinetic parameters may help to explain and predict K_v11.1-mediated cardiotoxicity.

Introduction

Cardiac safety has become a major concern facing the pharmaceutical industries and regulatory agencies over the last several decades. A substantial number of drugs, including both cardiac and non-cardiac medications, have been restricted in their applications or withdrawn from the market due to their K_v11.1-induced cardiotoxicity.[1, 2] The K_v11.1 channel, often referred to as the human ether-à-go-go-related gene (hERG) K^+ channel, mediates the most important component of phase 3 repolarization of human ventricular myocytes.[3] Blockade of the K_v11.1 channel can lead to the prolongation of action potential durations (APDs) and an elevated risk of lethal arrhythmias such as Torsade de Pointes (TdP).[4] As a consequence, measurement of K_v11.1 liability of drugs is a critical component of regulatory guidelines for preclinical QT studies.[5, 6] In this regard, a 30-fold safety margin between K_v11.1 IC_{50} and C_{max} values (maximum free plasma concentrations) has been proposed to define the cardiac safety of compounds.[7] However, this approach of considering IC_{50} values solely is rather arbitrary and crude, which might explain unsatisfactory quantitative predictions and sometimes excludes useful medications that are not problematic.[6, 8, 9] For instance, the IC_{50} value of ketoconazole (1-[4-(4-{[(2*R*,4*S*)-2-(2,4-Dichlorophenyl)-2-(1*H*-imidazol-1-ylmethyl)-1,3-dioxolan-4-yl] methoxy}phenyl)piperazin-1-yl]ethan-1-one) at the K_v11.1 channel is relatively close to its effective therapeutic plasma concentration (11-fold difference), yet it has been proven to be a safe drug in clinical trials due to the fact that this drug has a slow binding rate and is not trapped into the channel.[9, 10] Therefore, knowledge of association and dissociation kinetics of drugs at the K_v11.1 channel may be important in defining their propensities to prolong the QT interval.

The concept of structure-affinity relationships (SARs) describing the interdependency between compound structures and binding affinity has been extensively explored over the past decades.[11, 12] However, similar studies illustrating the dependency between compound structures and binding kinetics, coined as structure-kinetics relationships (SKRs), have been less well investigated to date. Recently, drug-target kinetics, in particular receptor-ligand residence times (RTs), have been shown to also determine the therapeutic potential of drug candidates *in vivo*, and to be predictive of drug efficacy and safety.[13, 14] Consequently, there is an emerging awareness of the importance of measuring the kinetics of drug-target interactions. SKRs are now being reported and discussed for ligand binding to G protein-coupled receptors (GPCRs) and enzymes.[11, 15-17] With regard to ion channels, measuring the interaction kinetics of drugs with the K_v11.1 channel has already been recommended to be incorporated into Comprehensive *in vitro*

Proarrhythmia Assay (CiPA) strategies to hopefully provide significant improvements of proarrhythmic assessments.[18, 19] Recent studies have demonstrated that K_v11.1 blockers with similar potency (IC_{50} values) but distinct binding kinetics can have markedly diverse proarrhythmic potential, suggesting the necessity to extend K_v11.1 inhibition assays with studies on investigating the dynamics of drug-channel interactions.[1, 8, 9] In addition, particular interest has arisen in the so-called trapping phenomenon, characterized by capture of a drug within the K_v11.1 channel and thus a slow dissociation rate from the channel, which harbors an enhanced proarrhythmic risk caused by the drug.[20, 21] Moreover, a substantial underestimation of cardiac risks has been observed in assessing the ventricular action potential due to neglecting drug-binding kinetics at cardiac K_v11.1 channels.[8] Therefore, there is an urgent need to add the dimension of binding and unbinding kinetics to the more routinely determined affinity values in order to evaluate the arrhythmogenic potential of drug candidates *in vitro*.

In our previous studies, we have successfully validated a [^{3}H]dofetilide competition association assay that can determine the association/dissociation rates and RTs of compounds accurately and efficiently.[2] In the present study a structurally diverse set of K_v11.1 blockers with four different scaffolds were newly synthesized or selected from our in-house library published previously,[22-25] and their kinetic parameters (k_{on}, k_{off}, K_D and RTs) as well as affinity (K_i) were determined in [^{3}H]dofetilide binding assays. A k_{on}-k_{off}-K_D 'kinetic map' was delineated for all compounds together with three reference compounds: astemizole (1-[(4-fluorophenyl)methyl]-N-[1-[2-(4-methoxyphenyl)ethyl]-4-piperidyl]benzoimidazol-2-amine, a notorious K_v11.1 blocker), dofetilide (N-[4-(2-{[2-(4-methane sulfonamidophenoxy)ethyl] (methyl)amino}ethyl)phenyl]methanesulfonamide, a specific K_v11.1 blocker with restricted usage in the market) and ranolazine ((*RS*)-N-(2,6-dim-ethylphenyl)-2-[4-[2-hydroxy-3-(2-methoxyphenoxy)-propyl] pipe-razin-1-yl]acetamide, a safe K_v11.1 blocker).[2, 26-28] Two compounds were further tested in a manual patch clamp assay. The SARs and SKRs derived for the compounds in this study reveal new features and aspects of the blockers' interactions with the K_v11.1 channel. This information is expected to provide valuable information for circumventing K_v11.1-induced cardiotoxicity during the preclinical stages of the drug discovery pipeline.

Results and discussion

Chemistry

Compounds **19**, **20**, **24**, **25**, **27-30** and **39-46** were newly synthesized in order to

obtain compounds with various RT values besides a diverse range of K_i and k_{on} values. All other compounds were selected from our in-house library based on their distinct affinity and kinetic parameters, and synthesis of these compounds has been reported in our previously published studies.[22-25]

As shown in **Scheme 1**, clofilium (4-(4-Chlorophenyl)butyl-diethyl-heptylammonium) derivatives **19** and **20** were prepared from 4-iodotoluene in a 3-step sequence as following: Sonogashira cross-coupling of 4-iodotoluene and propargyl alcohol, formation of the corresponding tosylate and displacement of the tosylate with the corresponding secondary amine.[24]

Scheme 1. Synthesis of clofilium derivatives (**19** and **20**)

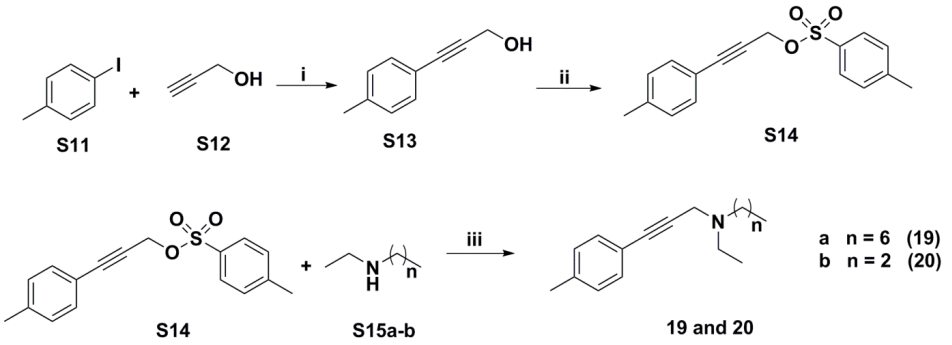

i) $PdCl_2(PPh_3)_2$, CuI, Et_3N, THF, r.t.; ii) tosyl chloride, KOH, Et_2O, 0 °C to r.t.; iii) K_2CO_3, DMF, r.t.

To investigate the effect of flexibility in the side chains of aliphatic pyridinium derivatives, several symmetrical 2,6-substituted *N*-methylated-pyridine compounds with different alkyl chain lengths (**24**, **25** and **27-30**) were synthesized according to **Scheme 2**. The first series of compounds (**S23a-e**) were derived from commercially available 2,6-dibromo-pyridine and 1-alkynes with various lengths via a Sonogashira coupling reaction.[25] The final compounds (**24, 25** and **27-29**) were synthesized in relatively high yields by reduction of triple bonds to single bonds and methylation of neutral pyridines. **30** was obtained directly from **S23e** by methylation of the central nitrogen with a good yield of 94%.

Next, influences of different substituents at the phenyl rings on affinity and kinetic parameters of K_v11.1 blockers were explored, and a series of substituted biphenyl pyridines (**39-46**) were synthesized. As displayed in **Scheme 3**, compound **S32** was obtained by Sonogashira reaction of 2,6-dibromo-pyridine and ethynyltrimethylsilane with $Pd(PPh_3)_4$ and CuI as catalysts instead of $PdCl_2(PPh_3)_2$ and CuI displayed in **Scheme 2**.[29] After one-pot deprotection and Castro-Stephens coupling with 1-bromo-4-iodobenzene,[30] **S32** was converted to **S33** in a low yield that was probably caused by formation of undesired oxidative

Scheme 2. Synthesis of symmetrical 2,6-substituted *N*-methylated pyridines with various alkyl chain lengths

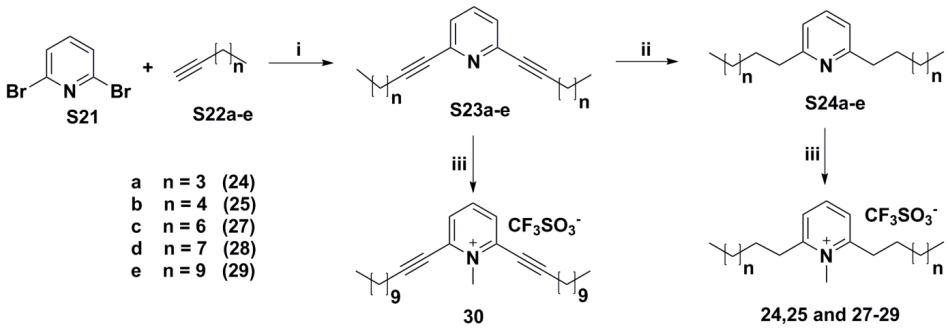

i) $PdCl_2(PPh_3)_2$, CuI, Et_3N, r.t.; ii) 10% Pd/C, H_2, THF, MeOH, r.t.; iii) $CF_3SO_2OCH_3$, CH_2Cl_2, 0 °C to r.t.

Scheme 3. Synthesis of symmetrical 2,6-substituted *N*-methylated pyridines with different biphenyl substituents

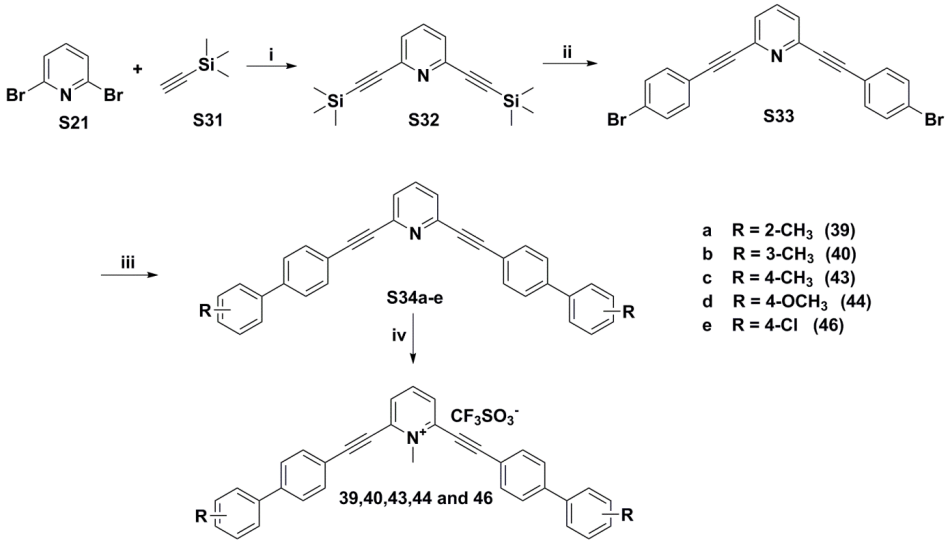

A) Synthesis of compounds **39, 40, 43, 44** and **46**: i) $Pd(PPh_3)_4$, CuI, diisopropylamine, toluene, r.t.; ii) CuCl ,PPh_3, potassium benzoate, 1-bromo-4-iodobenzene, DMI, 120 °C; iii) $Pd(PPh_3)_4$, K_2CO_3, toluene, ethanol, substituted-phenylboronic acid, 50 °C; iv) $CF_3SO_2OCH_3$, CH_2Cl_2, 0 °C to r.t.

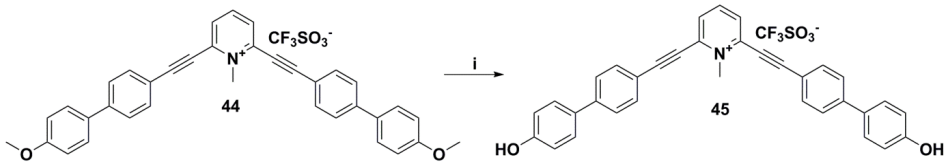

B) Synthesis of compound **45**: i) BBr_3, CH_2Cl_2, -78 °C to r.t.

Glaser homo-coupling and intra-polymerization of reacting molecules.[31] Suzuki reactions were further performed with **S33** and different substituted phenylboronic acids to yield the neutral pyridine compounds (**S34a-e**),[32] from which final compounds (**39**, **40**, **43, 44** and **46**) were derived via methylation of the central nitrogen in moderate to high yields. Subsequently, demethylation of **44** with boron tribromide led to the formation of compound **45**. Notably, synthetic routes mentioned above were not suitable for producing neutral biphenyl pyridines with methoxy and chlorine substituents at the meta-position of the second benzene ring. Hence, **41** and **42** were synthesized by different methods shown in **Scheme 4**. In the first step, Suzuki reactions were applied between the substituted phenylboronic acid and 1-bromo-4-iodobenzene in the presence of different palladium catalysts to produce **S43a** and **S43b** in moderate yields of 27% and 40%, respectively. **S43a** and **S43b** further reacted with ethynyltrimethylsilane through Sonogashira reaction,[33] resulting in high yields of **S44a** and **S44b**. Compound **41** was eventually obtained from **S44a** with a yield of 36% through three steps: deprotection, Sonogashira reaction and methylation, whereas **42** was obtained from **S44b** via a one-pot Sonogashira reaction and methylation in a yield of 45%.

Scheme 4. Synthesis of symmetrical 2,6-substituted *N*-methylated pyridines (**41** and **42**)

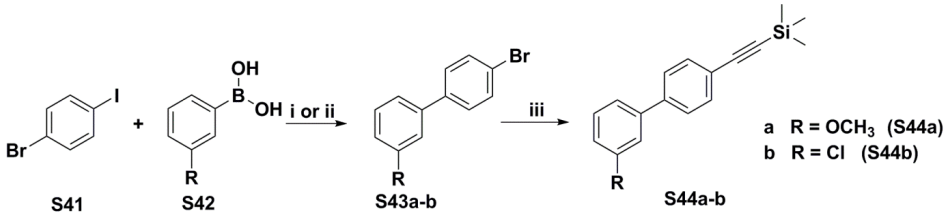

A) Synthesis of compounds **S44a-b**: i) 2M K_2CO_3, $Pd(PPh_3)_4$, toluene, ethanol, 80 °C; ii) 2M K_2CO_3, $Pd(OAc)_2$, PPh_3, toluene, ethanol, 80 °C; iii) $PdCl_2(PPh_3)_2$, CuI, PPh_3, THF, piperidine, 120 °C.

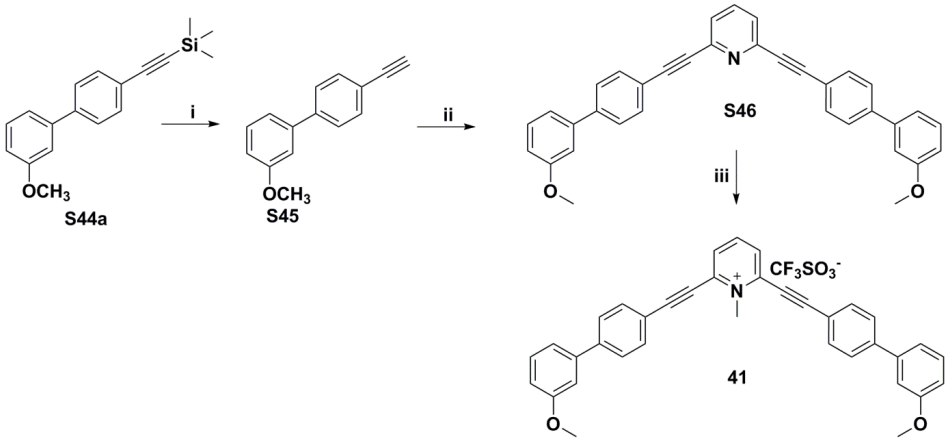

B) Synthesis of compound **41**: i) 2M NaOH, diethyl ether, methanol; ii) $PdCl_2(PPh_3)_2$, CuI, Et_3N, 2, 6-dibromo-pyridine; iii) $CF_3SO_2OCH_3$, CH_2Cl_2, 0 °C to r.t.

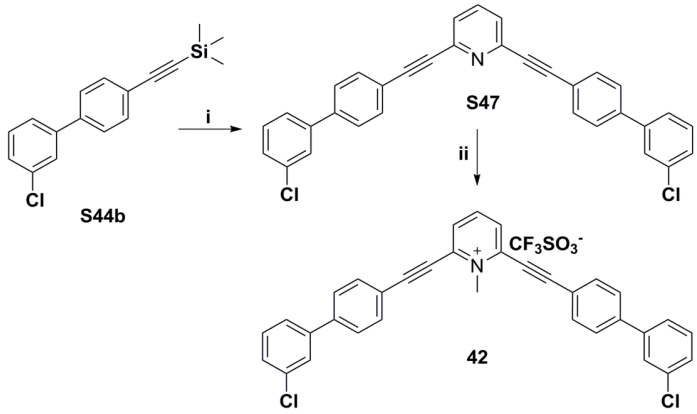

C) Synthesis of compound **42**: i) CuCl, PPh_3, potassium benzoate, 2, 6-dibromo-pyridine, DMI, 120 °C; ii) $CF_3SO_2OCH_3$, CH_2Cl_2, 0 °C to r.t.

Biology

The binding affinity and kinetic parameters of all compounds were determined in [^{3}H]dofetilide competitive displacement and competition association assays on HEK293 cell membranes stably transfected with the K_v11.1 channel (HEK-293K_v11.1) as described previously by our group.[2] As shown in **Figure 1**, compounds with a wide range of IC_{50} values demonstrated a monophasic binding behavior instead of a biphasic pattern reported for a [^{3}H]astemizole binding assay,[23, 25] indicating that the binding process of compounds followed a single-step bimolecular interaction scheme, and thus, fulfilled the theoretical requirements

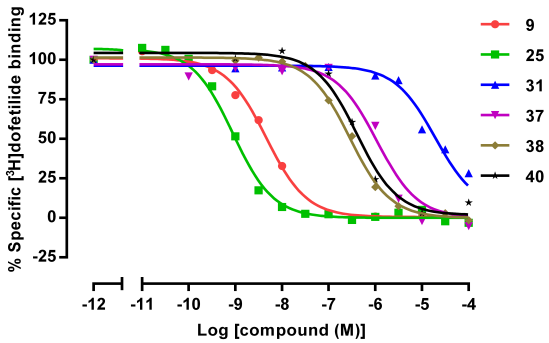

Figure 1. Representative displacement curves of specific [^{3}H]dofetilide binding by **9**, **25**, **31**, **37**, **38** and **40**. Experiments were performed at 25 °C using 20 µg of HEK293K_v11.1 membrane protein.

for the Motulsky-Mahan approach to evaluate the binding kinetics of unlabeled ligands.[34] **Figure 2** shows the competition association assay for three representative compounds (**31**, **37** and **38**) with different binding kinetics, in particular varying RTs. Compound **37** had a shorter RT than [^{3}H]dofetilide with an association curve slowly and monotonically approaching equilibrium versus time, whereas **38** possessed a longer RT compared to the radioligand, indicated by a typical 'overshoot' and then a decline in the association curve.[15] Meanwhile, **31** exhibited a RT similar to dofetilide, evidenced by the same curve shape compared to the association curve of radioligand alone. As the K_i values of all tested compounds calculated from the IC_{50} values mentioned above,[35] were in good agreement with kinetically derived K_D data ($K_D = k_{off}/k_{on}$, **Figure 3A**), only K_i values were used to summarize the SARs in this study. The consistency of K_i and K_D values extended our previous finding to a more general observation,[2] proving the reliability of the [^{3}H]dofetilide competition association assay in assessing the kinetics of unlabeled ligands at the K_v11.1 channel. In addition, the k_{on} values for all ligands were significantly correlated to their K_i values ($P < 0.0001$, **Figure 3B**), which is in agreement with our published data.[2] In the same publication affinity and kinetic parameters of the parental compounds dofetilide, E-4031 and clofilium were also measured and reported.[2] Furthermore, a provisional k_{on}-k_{off}-K_D 'kinetic map' was constructed based on the compounds' varying affinity and kinetic parameters in order to divide these compounds into four different groups (quadrants) of potentially negligible (quadrant **IV**), moderate (quadrant **I** and **III**) and high arrhythmic (quadrant **II**) side effects (**Figure 4**). Finally, we selected two compounds (**21** and **38**) with comparable binding affinity but distinct association and dissociation rates or RTs to be studied in a whole-cell patch clamp assay using the same HEK-293K_v11.1 cells (**Figure 5**).

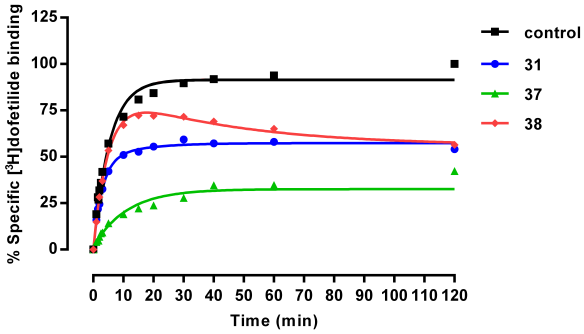

Figure 2. Representative competition association curves of [^{3}H]dofetilide in the absence (control) or presence of unlabeled **31**, **37** and **38** at their IC_{50} value concentrations. Experiments were performed at 25 °C using 20 µg of HEK293K_v11.1 membrane protein.

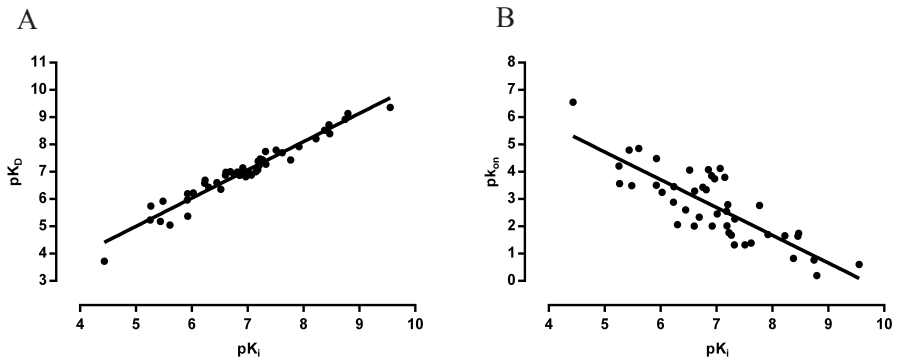

Figure 3. Correlation between pK_i and pK_D (**A**, $r^2 = 0.95$, $P < 0.0001$) or pk_{on} (**B**, $r^2 = 0.68$, $P < 0.0001$) values of all tested compounds as obtained from [^{3}H]dofetilide competitive displacement experiments and competition association assays, respectively.

Structure-affinity relationships (SARs) and structure-kinetics relationships (SKRs)

Derivatives of dofetilide

First, we explored the effects of pK_a values of the central nitrogen on affinity, association rates and RTs of compounds **1-8** (**Table 1**), in which the pK_a values were taken from our previous publication.[22] Briefly, increasing the pK_a values via different *N*-alkyl substituents resulted in an increase of affinity of these compounds (**1-5**, **7** and **8**) at the K_v11.1 channel. Association rates of these compounds were less sensitive to pK_a alterations but showed a similar trend as the affinity. For instance, compound **8** (pK_a = -4.95) displayed the lowest affinity and smallest k_{on} value, while **3** (pK_a = 9.61) had the highest affinity and fastest association rate at the channel. These changes corresponded rather well with the principle that reducing pK_a values of the central nitrogen of K_v11.1 blockers decreases the proportion of molecules in the protonated form at physiological pH and further make fewer active species available for the productive π-cation interactions with amino acid Tyr652 lining the inner cavity of the channel.[36, 37] Additionally, zwitterionic compound **6** with a CH_2COOH substituent at the central nitrogen had a lower affinity and slower association rate than **8**, indicating that the negatively charged carboxylate group caused unfavorable interactions of the K_v11.1 blocker with the channel.[38] Overall, however, the RTs ($1/k_{off}$) of **1-8** were not much impacted by pK_a values of the central nitrogen and zwitterionic propensity of molecules, with values between 0.56 ± 0.06 (**7**) and 3.8 ± 1.0 min (**3**).

Table 1. Binding affinity and kinetic parameters of dofetilide derivatives

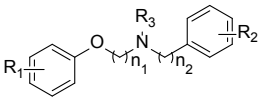

Compd	R_1	R_2	R_3	n_1	n_2	K_i (nM)	k_{on} ($nM^{-1}\cdot min^{-1}$)	k_{off} (min^{-1})	K_D (nM)	RT (min)
1	4-NO_2	4-NO_2	H	2	2	47±1	0.0054±0.0015	0.27±0.06	53±6	3.7±0.8
2	4-NO_2	4-NO_2	CH_3	2	2	24±2	0.041±0.004	0.82±0.09	20±4	1.2±0.1
3	4-NO_2	4-NO_2	CH_2CH_3	2	2	4.2±0.5	0.15±0.06	0.26±0.07	3.0±0.2	3.8±1.0
4	4-NO_2	4-NO_2	CH_2CH_2F	2	2	65±13	0.0096±0.0019	0.30±0.08	41±11	3.3±0.9
5	4-NO_2	4-NO_2	CH_2CN	2	2	203±6	0.0046±0.0012	0.40±0.05	99±26	2.5±0.3
6	4-NO_2	4-NO_2	CH_2COOH	2	2	588±31	0.0013±0.0001	0.35±0.10	260±52	2.9±0.8
7	4-NO_2	4-NO_2	$COCH_3$	2	2	251±32	0.0098±0.0034	1.8±0.2	132±5	0.56±0.06
8	4-NO_2	4-NO_2	$COCF_3$	2	2	355±14	0.0025±0.0003	0.61±0.09	247±27	1.6±0.3
9	4-NO_2	4-NO_2	CH_3	4	2	1.6±0.3	0.64±0.29	0.26±0.05	0.73±0.39	3.8±0.7
10	4-NO_2	4-NO_2	CH_3	4	1	66±6	0.0028±0.0008	0.22±0.05	85±7	4.5±1.0
11	3, 4-di-Cl	3, 4-di-Cl	CH_3	2	2	5571±507	$(6.2\pm3.0)\times10^{-5}$	0.19±0.01	5807±228	5.3±0.2
12	H	4-OCH_3	CH_3	2	2	944±58	$(5.6\pm0.9)\times10^{-4}$	0.30±0.07	591±197	3.3±0.7

Next, the lengths of side alkyl linkers and substituents on the phenyl rings were investigated for the analysis of SARs and SKRs. Comparable to our own studies on distance-related flexibility,[24, 39] elongation of the alkyl chain between the central nitrogen and phenoxy moiety enhanced the K_v11.1 affinity and association rates (**9** versus **2**), while shortening the other alkyl linker with the phenyl ring lowered the affinity and association rates (**10** versus **2** and **9**). Nonetheless, **9** (RT = 3.8 ± 0.7 min) and **10** (RT = 4.5 ± 1.0 min) demonstrated similar dissociation characteristics at the K_v11.1 channel compared to other compounds in **Table 1**, suggesting that varying chain lengths between the central nitrogen and the two peripheral aromatic rings exerted negligible effects on the dissociation process of this type of ligands from the K_v11.1 channel. In addition, replacement of NO_2 groups on the phenoxy and phenyl rings with 3,4-di-Cl or other groups like OCH_3 dramatically decreased the K_v11.1 affinity and association rates of ligands (**11** and **12** versus **2**). Compound **11** had the lowest affinity (K_i = 5571 ± 507 nM), slowest association rate (k_{on} = 6.2 ± 3.0)×10^{-5} $nM^{-1}\cdot min^{-1}$) but longest RT of 5.3 ± 0.2 min at the K_v11.1 channel amongst all dofetilide derivatives (**1**-**12**). This implies that addition of electron-withdrawing groups on the aromatic rings reduces the affinity and association kinetics of K_v11.1 blockers by hampering their π-stacking and hydrophobic interactions with Phe656 and Tyr652 residues lining the pore cavity of the K_v11.1 channel,[36, 40] whereby this hindered interaction did not obviously disturb the dissociation of ligands. Overall, the association rates of this series of compounds were (negatively) correlated to their K_i values (see also **Figure 3B**), which is in full agreement with our previous finding that ligand affinity for the

K_v11.1 channel are mainly regulated by the compounds' association rates.[2] Unlike the widely varying K_i and k_{on} values, RTs of these dofetilide analogues were largely similar.

Derivatives of E-4031

Benzoylpiperidine analogues (**13**, **14** and **16**) demonstrated comparable K_i and k_{on} values at the K_v11.1 channel. This implicates that: i) electron withdrawing or donating groups at the two peripheral rings, ii) slightly lengthening the carbon chain between the central nitrogen atom and the phenyl ring and iii) permanent protonation of the basic nitrogen, had much smaller effects on K_v11.1 affinity and association kinetics of E-4031 (N-[4-[1-[2-(6-Methylpyridin-2-yl)ethyl]piperidine-4-carbonyl]phenyl]) derivatives (**Table 2**) compared to the dofetilide series (**Table 1**). However, when the benzoylpiperidine was replaced by benzoylpiperazine (**15**), the K_i value was drastically increased to 5418 ± 374 nM and its association rate was substantially decreased to $(2.7 \pm 0.6)\times10^{-4}$ $nM^{-1}\cdot min^{-1}$. Distinct from the variations in affinity and association rates, all E-4031 derivatives displayed comparably short RTs between 2.0 ± 0.5 (**14**) and 2.9 ± 0.8 min (**16**) at the K_v11.1 channel.

Table 2. Binding affinity and kinetic parameters of E-4031 derivatives

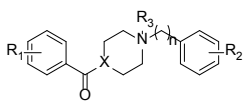

Compd	R_1	R_2	X	R_3	n	K_i (nM)	k_{on} ($nM^{-1}\cdot min^{-1}$)	k_{off} (min^{-1})	K_D (nM)	RT (min)
13	4-Cl	3, 4-di-Cl	CH	-	2	54±3	0.021±0.009	0.39±0.06	36±22	2.6±0.4
14	4-CH_3	H	CH	-	3	60±2	0.017±0.003	0.49±0.12	34±14	2.0±0.5
15	H	H	N	-	2	5418±374	$(2.7\pm0.6)\times10^{-4}$	0.46±0.03	1812±313	2.2±0.1
16	4-Cl	H	CH	CH_3	2	48±1	0.048±0.022	0.35±0.09	18±9	2.9±0.8

Derivatives of clofilium

Comparable to our own and other studies,[24, 25, 41] increasing the rigidity by introduction of alkene and alkyne moieties in the chain between the phenyl ring and central nitrogen atom diminished the K_v11.1 affinity and association rates of clofilium derivatives (**18** and **21** versus **17**, **Table 3**), whereby permanent protonation of the central nitrogen atom with a CH_2CH_3 group resulted in a dramatic enhancement of the affinity and association rate (K_i = 1.8 ± 0.2 nM and k_{on} = 0.17 ± 0.07 $nM^{-1}\cdot min^{-1}$ for **22**). Therefore, rigidity and protonation play pivotal roles in determining the affinity and association rates of clofilium analogues at

the K_v11.1 channel. However, permanently protonating the central nitrogen obviously imposed more significant effects on K_v11.1 affinity and association rates, and thus compensated for the negative influences exerted by increasing rigidity via introduction of an alkyne bond (**22** versus **17**). According to different in-silico K_v11.1 models, protonation of the central nitrogen atom facilitates the π-cation interaction of ligands with the crucial binding residue (Tyr652) that faces into the S6 domain of the channel.[36, 42-44] With regard to dissociation characteristics, compounds **17** and **18** had similar RTs at the K_v11.1 channel (2.7 ± 0.3 and 2.0 ± 0.5 min for **17** and **18**, respectively), while **21** and **22** having an alkyne moiety displayed longer RTs. Subsequently, two novel compounds with an alkyne group but different side chain lengths (**19** and **20**) were synthesized in order to obtain more variations in dissociation rate constants or RTs. Both compounds exhibited comparably low affinity and slow association rates at the K_v11.1 channel, indicating the flexibility adjusted by side chain lengths imposed insignificant effects on weakening K_v11.1 affinity and association kinetics of this series of ligands. Likewise, the dissociation rates of **19** and **20** were identical with comparatively longer RTs of 7.7 ± 1.6 and 6.7 ± 2.0 min, respectively. Altogether, introduction of an alkyne group in these clofilium analogues slightly increased their RTs at the K_v11.1 channel (**19-22** versus **17-18**). With all these clofilium derivatives (**Table 3**), their association rates illustrated the same overall tendency as the affinity shown in **Figure 3B**. Most importantly, compound **22** showed the highest affinity, fastest association rate and longest RT, implying a strong and prolonged inhibition of the K_v11.1channel.

Table 3. Binding affinity and kinetic parameters of clofilium derivatives

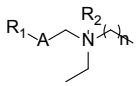

Compd	R_1	R_2	A	n	K_i (nM)	k_{on} ($nM^{-1}\cdot min^{-1}$)	k_{off} (min^{-1})	K_D (nM)	RT (min)
17	4-Cl-$C_6H_4CH_2$	-	—CH_2CH_2—	6	31±5	0.048±0.019	0.37±0.04	16±10	2.7±0.3
18	$C_6H_5CH_2$	-	-HC:CH-	6	119±2	0.0098±0.0042	0.50±0.12	86±45	2.0±0.5
19	4-CH_3-C_6H_5	-	—C≡C—	6	3282±613	(3.2±2.0)x10^{-4}	0.13±0.03	1188±122	7.7±1.6
20	4-CH_3-C_6H_5	-	—C≡C—	2	1196±141	(3.1±0.7)x10^{-4}	0.15±0.05	637±339	6.7±2.0
21	$(C_6H_5)_2CH$	-	—C≡C—	6	97±13	0.0035±0.0008	0.27±0.06	100±52	3.7±0.8
22	4-Cl-C_6H_5	CH_2CH_3	—C≡C—	6	1.8±0.2	0.17±0.07	0.13±0.04	1.2±0.6	7.7±2.6

Derivatives of pyridinium

As compounds with high lipophilicity can bind to residue Phe656 of the K_v11.1 channel through hydrophobic van der Waals interactions as well, peripheral aro-

maticity is not essential for their K_v11.1 binding.[25, 37] In this context, eight aliphatic pyridinium analogues with various side chains (**23-30**) were synthesized or selected to define their SARs and SKRs (**Table 4**). Several general observations can be made: i) permanently protonating the central nitrogen atom by a methyl substituent (**23** versus other compounds), and ii) increasing flexibility via stretching the side alkyl chain from n = 3 to n = 6 (**24** versus **25-27**) enhanced the K_v11.1 affinity of compounds. However, the binding affinity were decreased with iii) the continuous prolongation of side chains up to n=7 (**24** versus **28-29**) and iv) replacement of alkane with alkyne (**29** versus **30**). All these results are in excellent agreement with protonation and rigidity rules,[45] and with the fact that the large aperture at the bottom of the K_v11.1 channel cavity has boundaries that accommodate molecules with defined sizes.[46] Likewise, protonation, flexibility of side chains and rigidity by an alkyne moiety exerted the same overall effects on association rates of these aliphatic pyridines, which implicates that the affinity of aliphatic pyridinium blockers were correlated to their association rate constants at the K_v11.1 channel (see also for dofetilide, E-4031 and clofilium derivatives, **Figure 3B**). Intriguingly, RTs in this series of compounds tended to be longer and different from the three other compound classes mentioned above as well as from our previous data.[2] The newly synthesized compound **29** had the longest RT of 36 ± 2 min, whereas **24** showed the shortest RT with 4.3 ± 0.8 min. In addition, pyridines with *n*-octyl side chains (**23**, RT = 19 ± 1 min) presented a comparable RT to **26** (25 ± 1 min) and **28** (16 ± 4 min) at the K_v11.1 channel. Apparently, permanent protonation of the central nitrogen atom (**23** versus **26**) and prolongation of side alkyl chains (**28** versus **23** and **26**) had much less influence on RTs compared to their roles in overall affinity and association rates. It is noteworthy that more rigidity induced by an alkyne moiety diminished the RT to 8.3 ± 1.7 min for **30**. Altogether, increasing rigidity of aliphatic pyridine blockers can decrease their affinity, association rates and RTs simultaneously (**30** versus **29**), and thus, it may provide an efficient solution for circumventing K_v11.1 side effects of drug candidates. In a second series of pyridinium analogues (**31-33**), the K_v11.1 affinity and association rates were also increased by permanent protonation of the central nitrogen atom (**32** versus **31**) but decreased with an alkyne moiety (**33** versus **32**). However, the RTs of **31-33** were comparable between 7.7 ± 0.7 (**32**) and 9.1 ± 1.7 min (**33**), indicating different dissociation profiles of these compounds compared to aliphatic pyridinium analogues of which rigidity affected the RTs significantly.

Next, a series of biphenyl substituted pyridinium derivatives (**34**, **35** and **38-46**) together with their precursors (**36** and **37**) were synthesized or selected to achieve more variations in RTs. As shown in **Table 4**, permanent protonation and rigidification by alkyne imposed the same effects on K_v11.1 affinity as our

findings for other derivatives (**34** versus **35-46** and **35** versus **36-46**, respectively**)**. Additionally, decreasing bulkiness via removal of the second benzene rings or replacing the aromatic phenyl rings close to the central nitrogen atom with cyclohexyl diminished the affinity of K_v11.1 blockers (**36-37** versus **38**), possibly caused by reduced π-stacking and hydrophobic interactions.[36] Furthermore, introduction of different groups at the second benzene rings lowered their K_v11.1 affinity compared to the non-substituted compound (**39-45** versus **38**), indicating a possible steric hindrance of these groups in ligand binding.[22, 25] Although the k_{on} values showed a comparable decline to affinity because of the increased rigidity by an alkyne moiety (**35** versus **38-46**) and reduction of the aromatic rings (**36** versus **37**), the negative relationship between K_i and k_{on} values was not conspicuous for this series of compounds. For instance, compound **38** showed a smaller K_i value as well as slower association rate than **39**. On the contrary, the RTs of these compounds were significantly increased by replacing ethyl with alkyne (**35** versus **38-46)**. Moreover, decreasing bulkiness of these pyridinium analogues led to shorter RTs (**36-37** versus **38-46**). Compound **36** and **37** showed the shortest RTs amongst all these derivatives, providing evidence that reduced bulkiness facilitates unbinding dynamics of K_v11.1 blockers at the channel. Our findings are contradictory to the classic 'foot-in-door' mechanism, in which bulky residues of K_v11.1 blockers prevent the closure of the channel gate and thus promote the channel recovery from blockade.[20] The explanation for our results is that less hydrophobic interactions and smaller sizes of molecules can accelerate the dissociation of such ligands from the channel. Compound **38** without any substituents on the benzene rings had the longest RT of 105 ± 4 min at the K_v11.1 channel, while substituents at the second benzene rings (**39-46**) often had distinct and lowering effects on RTs. While introducing CH_3 (**40**) and Cl (**42**) at the meta-position did not affect RTs significantly, a substituent at the ortho-position (**39**) of the benzene rings reduced the RT, like at the para-position (**43-46**) but to a lesser extent (**43** versus **39**). Secondly, a methoxy group at the meta-position of the second benzene rings was less favorable for maintaining long RTs (**41** versus **40** and **42)**. A similar observation was made for the two compounds with 4-OCH_3 (**44**) and 4-OH (**45**) groups at the second benzene rings, of which RTs were decreased to 24 ± 4 and 19 ± 3 min, respectively, particularly when compared with **46** (63 ± 4 min) and **43** (30 ± 6 min). Collectively, we have successfully obtained compounds with divergent RTs (i.e. approx. 300-fold difference, between **37** and **38**) next to varied affinity and association rates, which provides the possibility to investigate the influence of RTs on *in vivo* cardiotoxicity of K_v11.1 blockers.

Table 4. Binding affinity and kinetic parameters of pyridinium analogues

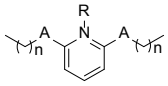

Compd	A	R	n	K_i (nM)	k_{on} ($nM^{-1}\cdot min^{-1}$)	k_{off} (min^{-1})	K_D (nM)	RT (min)
23	—CH_2CH_2—	-	5	36870±10861	(2.8±0.4)x10^{-7}	0.052±0.002	190546±27585	19±1
24	—CH_2CH_2—	CH_3	3	12±1	0.020±0.005	0.23±0.04	12±0	4.3±0.8
25	—CH_2CH_2—	CH_3	4	0.28±0.01	0.25±0.08	0.10 ± 0.02	0.44±0.05	10± 2
26	—CH_2CH_2—	CH_3	5	3.5±0.3	0.023±0.004	0.040±0.002	1.9±0.5	25±1
27	—CH_2CH_2—	CH_3	6	3.4±0.9	0.018±0.003	0.069±0.005	4.0±0.6	14±1
28	—CH_2CH_2—	CH_3	7	17±3	0.0017±0.0002	0.064±0.015	37±5	16±4
29	—CH_2CH_2—	CH_3	9	108±10	(1.8±0.2)x10^{-4}	0.028±0.001	153±10	36±2
30	—C≡C—	CH_3	9	1179±297	(3.3±1.1)x10^{-5}	0.12±0.02	4258±1139	8.3±1.7

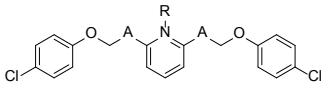

Compd	A	R	K_i (nM)	k_{on} ($nM^{-1}\cdot min^{-1}$)	k_{off} (min^{-1})	K_D (nM)	RT (min)
31	—CH_2CH_2—	-	3654±81	(1.6±0.3)x10^{-5}	0.11±0.01	6631±536	9.1±0.8
32	—CH_2CH_2—	CH_3	6.0±0.5	0.022±0.003	0.13±0.01	6.1±1.2	7.7±0.7
33	—C≡C—	CH_3	2460±262	(1.4±0.4)x10^{-5}	0.11±0.02	8877±1904	9.1±1.7

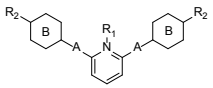

Compd	R_1	A	R_2	B	K_i (nM)	k_{on} ($nM^{-1}\cdot min^{-1}$)	k_{off} (min^{-1})	K_D (nM)	RT (min)
34	-	—C≡C—	C_6H_5	C_6H_4	>100 µM	n.d.	n.d.	n.d.	n.d.
35	CH_3	—CH_2CH_2—	C_6H_5	C_6H_4	63±9	0.0016±0.0003	0.098±0.021	60±4	10±2
36	CH_3	—C≡C—	H	C_6H_{10}	1208±36	(3.3±1.2)×10^{-4}	0.30±0.05	1074±268	3.3±0.6
37	CH_3	—C≡C—	H	C_6H_4	498±107	0.0086±0.0020	2.9±0.3	368±61	0.34±0.04
38	CH_3	—C≡C—	C_6H_5	C_6H_4	86±12	(7.5±1.0) ×10^{-5}	0.0095±0.0003	132±19	105±4
39	CH_3	—C≡C—	2-CH_3-C_6H_5	C_6H_4	577±41	(3.5±0.3)×1^{0}·4	0.071±0.004	203±19	14±1
40	CH_3	—C≡C—	3-CH_3-C_6H_5	C_6H_4	122±15	(1.4±0.2)×10^{-4}	0.010±0.003	72±18	100±30
41	CH_3	—C≡C—	3-OCH_3-C_6H_5	C_6H_4	176±10	(3.7±0.4)×10^{-4}	0.047±0.009	125±13	21± 4
42	CH_3	—C≡C—	3-Cl-C_6H_5	C_6H_4	139±20	(8.3±0.9)×10^{-5}	0.011±0.002	135±14	91±17
43	CH_3	—C≡C—	4-CH_3-C_6H_5	C_6H_4	303±49	(8.6±1.0)×10^{-5}	0.033±0.006	440±78	30±6
44	CH_3	—C≡C—	4-OCH_3-C_6H_5	C_6H_4	247±44	(4.5±0.2)×10^{-4}	0.042±0.007	105±16	24± 4
45	CH_3	—C≡C—	4-OH-C_6H_5	C_6H_4	153±32	(5.1±0.7)×10^{-4}	0.053±0.008	103±3	19±3
46	CH_3	—C≡C—	4-Cl-C_6H_5	C_6H_4	71±9	(1.6±0.2)×10^{-4}	0.016±0.001	100±10	63±4

n.d.: not detectable.

Kinetic map

Using the kinetic data in **Tables 1-4**, we plotted the dissociation rates (pk_{off}, y axis) against association rates (pk_{on}, x axis) of all our compounds together with three reference compounds (astemizole, dofetilide and ranolazine) into a kinetic map (**Figure 4**). The parallel diagonal dashed lines represent the kinetically derived K_D values. In this k_{on}-k_{off}-K_D map, compounds with the same affinity or association rates may have divergent dissociation rates or RTs, and vice versa. Therefore, risk assessment and possible mitigation of inhibitory efficacies of K_v11.1 blockers should take association rates (k_{on}) and RTs into account rather than affinity alone. In this context, all ligands were divided into four quadrants (**I**, **II**, **III** and **IV**) according to our hypothesis that high affinity, fast association rates and slow dissociation rates (long RTs) contribute together to serious K_v11.1-induced cardiotoxicity. The affinity and kinetic parameters of astemizole, dofetilide and ranolazine were derived from our previous investigation.[2] Astemizole was distributed into quadrant **II**, as it is a specific K_v11.1 blocker and has been withdrawn from the market.[26, 27] On the other hand, ranolazine was assigned to quadrant **IV,** since it inhibits the K_v11.1 channel but does not cause proarrhythmic events.[28] In addition, dofetilide is restrictedly used in the United States due to its low and finite TdP by blocking the K_v11.1 channel,[27, 47, 48] and consequently, it was scattered into quadrant **III**. Obviously, compounds in quadrant **II** have high affinity (K_D < 316 nM), fast association rates ($k_{on} > 3.2\times10^{-4}$ $nM^{-1}\cdot min^{-1}$) and slow dissociation rates or long RTs (> 10 min) at the K_v11.1 channel, indicating that they may cause serious arrhythmias via blockade of the channel. On the other hand, quadrant **IV** comprises compounds with low affinity (K_D > 316 nM), slow association rates ($k_{on} < 3.2\times10^{-4}$ $nM^{-1}\cdot min^{-1}$) and fast dissociation rates or short RTs (< 10 min) at the channel, suggesting their possible cardiac safety in terms of K_v11.1 inhibition. Quadrants **I** and **III** encompass moderately active K_v11.1 blockers with either relatively low affinity, slow k_{on} ($< 3.2\times10^{-4}$ $nM^{-1}\cdot min^{-1}$) and k_{off} (RT > 10 min, **I**) or comparatively high affinity, fast k_{on} ($> 3.2\times10^{-4}$ $nM^{-1}\cdot min^{-1}$) and k_{off} (RT < 10 min, **III**). Most likely these two different classes of compounds have modest K_v11.1-related cardiac side effects. Taken together, this arbitrary and provisional kinetic map that can be further extended with other suspected K_v11.1 blockers sheds light on K_v11.1-induced cardiotoxicity of drugs by bringing together their affinity as the traditional safety parameter with their kinetic parameters of association and dissociation rates (or RTs) at the channel. Therefore, a similar map would provide valuable information on how to accurately and comprehensively evaluate and further circumvent K_v11.1 liability of drug candidates in the future.

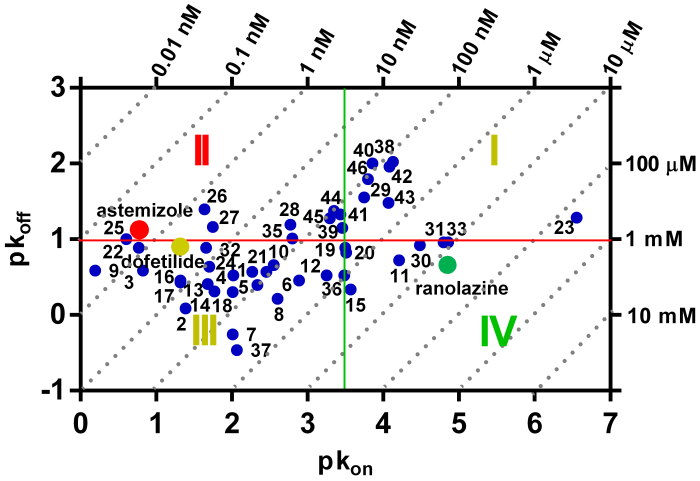

Figure 4. Kinetic map of all tested compounds in which the dissociation rate ($pk_{off,}$ k_{off}: min^{-1}) is plotted on the y axis, whereas the association rate ($pk_{on,}$ $k_{on:}$ $nM^{-1}\cdot min^{-1}$) is plotted on the x axis. Identical K_D values can result from different combinations of k_{on} and k_{off} values ($K_D = k_{off}/k_{on}$, diagonal dashed lines). Quadrants (**I**, **II**, **III**, **IV**) are arbitrarily defined by red horizontal and green vertical lines according to the varied k_{on}, k_{off} and K_D values in combination with three reference compounds astemizole (red dot), dofetilide (yellow dot) and ranolazine (green dot). The intersection of red and green lines are arranged on the diagonal dashed line representing a K_D value of 316 nM, while their intercepts with y and x axis are 1 (RT = 10 min) and 3.5 ($k_{on} = 3.2\times10^{-4}$ $nM^{-1}\cdot min^{-1}$), respectively. Note that the kinetic parameters of compound **34** could not be determined due to its rather low K_v11.1 affinity and thus is excluded in this map.

Patch clamp study

A whole-cell voltage patch clamp assay was applied to determine the functional hERG current blockade by **21** and **38**, two compounds with similar affinity but different RTs. As shown in **Figure 5A**, the IC_{50} values for **21** and **38** from their concentration-effect curves in the patch clamp assay were 182 ± 6 and 107 ± 6 nM, respectively. However, **21** and **38** had almost identical affinity in the radioligand binding assay with K_i values of 97 ± 13 and 86 ± 12 nM, respectively. RTs of ligands have been found to be correlated to their efficacies in functional assays rather than affinity at the adenosine A_{2A} receptor.[49] Thus, we surmised that the difference in IC_{50} values obtained in functional patch clamp assays for these two compounds might be caused by their different RTs, with **38** (long RT of 105 ± 4 min) displaying a higher potency in K_v11.1 current inhibition than **21** (short RT

of 3.7 ± 0.8 min). The time-dependent inhibition of the K_v11.1 current for **21** and **38** was also assessed in the whole-cell patch clamp assay. As shown in **Figure 5B**, compound **21** with a faster association rate (0.0035 ± 0.0008 $nM^{-1}\cdot min^{-1}$) in the radioligand binding assay almost completely inhibited K_v11.1 currents within 10 min, whereas 15 min was required for **38** (k_{on} = (7.5 ± 1.0)×10^{-5} $nM^{-1}\cdot min^{-1}$) to approach the equilibrated current inhibition. Therefore, association rates measured in the [^{3}H]dofetilide competition association assay may be linked to the current inhibition rates of compounds in the functional patch clamp experiments. Although different wash-in times for K_v11.1 blockers have been observed on an automated patch clamp platform before,[23] this is the first time to interpolate the radioligand binding parameters, especially for the association and dissociation rates, into functional data derived from patch clamp assays.

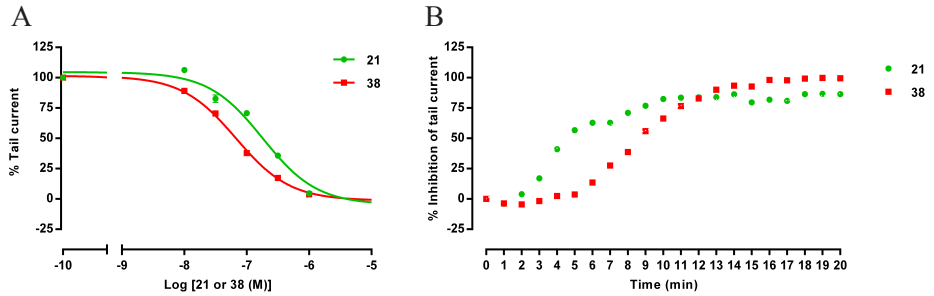

Figure 5. (A) Concentration-dependent inhibition of **21** and **38** for the K_v11.1 tail current in electrophysiological experiments. **(B)** Time-dependent inhibition of the K_v11.1 tail current by **21** and **38** (1 µM). Experiments were performed at room temperature using HEK293K_v11.1 cells.

Conclusion

Although affinity and association rates of compounds at the K_v11.1 channel have been found to differ vastly and are correlated to each other, this study is the first to verify that K_v11.1 blockers can possess very different RTs, with up to a more than 300-fold difference (**37** versus **38**) at the channel. Furthermore, this comprehensive investigation on derivatives of dofetilide, E-4031, clofilium and pyridinium over a range of scaffolds is the first to illustrate the impact of several parameters outlined above on association rates and RTs of compounds at the K_v11.1 channel in addition to their binding affinity. Notably, unlike the consistency of SARs for all compounds, SKRs are more chemical scaffold-dependent, in particular the structure-RT relationships. According to these findings and helped by the substantial differences in affinity, association and dissociation rate constants or RTs in the current sets of compounds, we delineated a k_{on}-k_{off}-K_D kinetic

map, and divided all these compounds into four quadrants (toxic for quadrant **II**, safe for quadrant **IV** and suspicious for quadrant **I** and **III** in **Figure 4**), which might provide valuable information for pharmaceutical researchers to devise better strategies for assessing K_v11.1 liability. Additionally, the association rates of two selected compounds were found to correspond well with their current block rates in the patch clamp studies, and their distinct RTs are a possible reason for their differences in functional potency when compared to their binding affinity. Although far from complete this analysis further indicates that kinetic parameters (k_{on} and RTs) should be taken into consideration as well as affinity (K_i) during the investigation of K_v11.1-mediated adverse reactions. To conclude, the new finding of large variations in RTs promotes the extensive analysis of structure-RT relationships, and the combination of SARs and SKRs opens a new avenue for medicinal chemists to more efficiently design new chemical entities with low or negligible K_v11.1-induced cardiotoxicity.

Experimental section

Chemistry

All commercially available chemicals and solvents were used without purification, except for ethyl acetate, which was distilled before usage. Demineralized water will be referred to as H_2O, unless otherwise stated. Reactions were monitored by thin-layer chromatography (TLC) using TLC silica gel 60 F254 aluminum sheets. TLC visualization was performed by a LAMAG UV-light at a wavelength of 254 or 366 nm. Grace Davison Davisil silica column material (LC60A 30-200 micron) was used for purification by column chromatography. ^{1}H and ^{13}C NMR spectra were recorded on a Bruker AV400 or AV600 spectrometer. Deuterated solutions $CDCl_3$, DMSO or MeOD were used for sample preparation. Chemical shifts (δ) are given in ppm and coupling constants (*J*) in Hertz. Trimethylsilane was used as internal standard for calibrating chemical shift for ^{1}H, ^{13}C NMR spectroscopy. HPLC-analysis was carried out on a Phenomenex Gemini reversed-phase C18 column (50 mm × 4.6 mm × 3 μm) coupled to a UV-detector at 254 nm. Final compounds were dissolved in either a mixture of acetonitrile:tert-butanol:water (1:1:1) or in pure acetonitrile and were eluted from the column at a flow rate of 1.3 $mL \cdot min^{-1}$ with 10/90 acetonitrile/water + 10% TFA, decreasing polarity of this mixture in time. LC-MS analysis was performed on an LCQ Advantage Max (Thermo Finnigan) ion-trap spectrometer (ESI^+) coupled to a Surveyor HPLC system (Thermo Finnigan) equipped with a C18 column (Phenomenex Gemini, 50 mm x 4.6 mm, 5 μm). A linear gradient of 10/90 acetonitrile/water + a constant

10% of an 1% TFA in water solution was used as the mobile system. The purity of all final compounds was > 95%. High-resolution mass spectral analysis (HRMS) was performed by Leiden Institute of Chemistry by direct injection (2 µL of a 2 µM solution in water/MeCN; 50/50; v/v and 0.1% formicacid) on a LTQ-Orbitrap FTMS operated in a positive ionization mode with an electrospray ionization (ESI) source (source voltage 3.5 kV, sheath gas flow 10%, capillary temperature 275 ˚C) with resolution R = 60000 at m/z 400 (mass range m/z = 150-2000) and calibrated for dioctylphthalate (m/z = 391.28428). All microwave reactions were performed in a Biotage initiator 2.5 in a sealed microwave vial.

3-(*P*-tolyl)prop-2-yn-1-ol (S13). To a solution of 4-iodotoluene (5.45 g, 25 mmol) in THF (33 mL) and Et_3N (7.3 mL) were added $PdCl_2(PPh_3)_2$ (35 mg, 0.5 mmol) and CuI (327 mg, 1.7 mmol). The mixture was stirred for 30 minutes and a solution of propargyl alcohol (1.48 mL, 25 mmol) in THF (10 mL) was added dropwise. The mixture was stirred at r.t. for 12 hours and filtered on Celite. The solvents were evaporated and the crude residue was purified by flash chromatography on silica gel (33% EtOAc-Petroleum ether) to afford pure **S13** (2.54 g, 70%) as an oil. Spectral data were in agreement with literature.[50]

3-(*P*-tolyl)prop-2-yn-1-yl 4-methylbenzenesulfonate (S14). To a stirred solution of **S13** (1 g, 6.8 mmol) in diethylether (45 mL) at 0 °C was added tosyl chloride (1.6 g, 8.2 mmol) followed, portionwise, by freshly powdered KOH (3.8 g, 68 mmol). After the addition was complete, the reaction mixture was stirred at room temperature for 3.5 h and then poured into water (90 mL). The layers were separated and the aqueous phase was extracted with EtOAc (3 × 40 mL). The combined organic extract was dried, filtered, concentrated *in vacuo* and chromatographed (25% EtOAc - Petroleum ether) to obtain the title compound **S14** (1.9 g, 91%). ^{1}H NMR (400 MHz, $CDCl_3$) δ 7.87 (d, *J* = 8.2 Hz, 2H), 7.34 (d, *J* = 8.2 Hz, 2H), 7.17 (d, *J* = 8.1 Hz, 2H), 7.11 (d, *J* = 8.1 Hz, 2H), 4.97 (s, 2H), 2.42 (s, 3H), 2.36 (s, 3H) ppm.

General Sonogashira coupling procedure (S23a-e).

$PdCl_2(PPh_3)_2$ (148 mg, 0.21 mmol, 0.05 eq.) and CuI (121 mg, 0.63 mmol, 0.15 eq.) was added to a solution of 2,6-dibromopyridine (1000 mg, 4.22 mmol, 1.0 eq.) in Et_3N (10 mL) and stirred for 30 min under a nitrogen atmosphere. The appropriate alkyne (10.1 mmol, 2.4 eq.) was added drop wise, and the mixture was stirred overnight at room temperature after which full conversion was shown by TLC. The reaction mixture was adsorbed on silica and purification by FCC yielded the desired compound.

2,6-di(hex-1-ynyl)pyridine (S23a). Prepared from hex-1-yne. FCC (petroleum ether: ethyl acetate 60:1 to 20:1) gave the desired product in a yield of (635

mg) 63%; ^{1}H NMR (400MHz, $CDCl_3$): δ 7.52 (t, *J* = 8.0 Hz, 1H), 7.25 (d, *J* = 8.0 Hz, 2H), 2.42 (t, *J* = 7.0 Hz, 4H), 1.64-1.56 (m, 4H), 1.52-1.42 (m, 4H), 0.93 (t, *J* = 7.4 Hz, 6H).

2,6-Di(hept-1-ynyl)pyridine (S23b). Prepared from hept-1-yne. FCC (petroleum ether:dichloromethane 4:1 tot 2:1) gave the desired product in a yield of (241 mg) 21%. ^{1}H NMR (400MHz, $CDCl_3$): δ 7.53 (t, *J* = 7.6 Hz, 1H), 7.25 (d, *J* = 7.6 Hz, 2H), 2.41 (t, *J* = 6.8 Hz, 4H), 1.64-1.60 (m, 4H), 1.44-1.31 (m, 8H), 0.91 (t, *J* = 7.2 Hz, 6H).

2,6-Di(non-1-ynyl)pyridine (S23c). Prepared from non-1-yne. FCC (petroleum ether:dichloromethane 30:1 tot 4:1) gave the desired product in a yield of (247 mg) 18%. ^{1}H NMR (400MHz, $CDCl_3$): δ 7.52 (t, *J* = 7.6 Hz, 1H), 7.25 (d, *J* = 8.0 Hz, 2H), 2.41 (t, *J* = 7.2 Hz, 4H), 1.65-1.57 (m, 4H), 1.45-1.39 (m, 4H), 1.35-1.26 (m, 12H), 0.89 (t, *J* = 6.4 Hz, 6H).

2,6-Di(dec-1-ynyl)pyridine (S23d). Prepared from dec-1-yne. FCC (petroleum ether:dichloromethane 5:1 to 3:1) gave the desired product in a yield of (210 mg) 14%. ^{1}H NMR (400MHz, $CDCl_3$): δ 7.53 (t, *J* = 8.0 Hz, 1H), 7.25 (d, *J* = 7.6 Hz, 2H), 2.41 (t, *J* = 7.2, 4H), 1.65-1.57 (m, 4H), 1.45-1.39 (m, 4H), 1.30-1.24 (m, 16H), 0.88 (t, *J* = 6.8 Hz, 6H).

2,6-Di(dodec-1-ynyl)pyridine (S23e). Prepared from dodec-1-yne. FCC (petroleum ether : dichloromethane 5:1 to 2:1) gave the desired product in a yield of 79% (1131 mg). ^{1}H NMR (400MHz, $CDCl_3$): δ 7.53 (t, *J* = 7.6 Hz, 1H), 7.25 (d, *J* = 8.0 Hz, 2H), 2.41 (t, *J* = 7.2 Hz, 4H), 1.64-1.57 (m, 4H), 1.44-1.39 (m, 4H), 1.32-1.26 (m, 24H), 0.88 (t, *J* = 6.4 Hz, 6H).

General procedure for reduction of pyridine alkynes (S24a-e).

The appropriate alkyne (**S23a**) (600 mg, 2.52 mmol) was dissolved in THF (3 mL) and MeOH (3 mL) under a N_2 atmosphere. 10% Pd/C (120 mg, 1.14 mmol) was added and H_2 was introduced via a balloon. The mixture was stirred overnight at r.t. after which the reaction mixture was filtered over Celite. The filtrate were concentrated under reduced pressure and FCC (petroleum ether:ethyl acetate 20:1) gave the desired compound.

2,6-Dihexylpyridine (S24a). Prepared from **S23a** and purified by FCC (petroleum ether:ethyl acetate 20:1) which gave the desired product in a yield of (469 mg) 75%. ^{1}H NMR (400MHz, $CDCl_3$): δ 7.48 (t, *J* = 7.6 Hz, 1H), 6.94 (d, *J* = 7.6 Hz, 2H), 2.75 (t, *J* = 7.6 Hz, 4H), 1.73-1.65 (m, 4H), 1.39-1.26 (m, 12H), 0.88 (t, *J* = 6.8 Hz, 6H).

2,6-Diheptylpyridine (S24b). Prepared from **S23b** and purified by FCC (petroleum ether:dichloromethane 4:1 to 1:2) which gave the desired product in a yield of (106 mg) 43%. ^{1}H NMR (400MHz, $CDCl_3$): δ 7.47 (t, *J* = 7.6 Hz, 1H),

6.93 (d, *J* = 7.6 Hz, 2H), 2.75 (t, *J* = 7.6 Hz, 4H), 1.71-1.66 (m, 4H), 1.34-1.23 (m, 16H), 0.87 (t, *J* = 6.8 Hz, 6H).

2,6-Dinonylpyridine (S24c). Prepared from **S23c** and purified by FCC (petroleum ether:dichloromethane 4:1 to 1:2) which gave the desired product in a yield of (91 mg) 78%. ^{1}H NMR (400MHz, $CDCl_3$): δ 7.47 (t, *J* = 7.6 Hz, 1H), 6.93 (d, *J* = 7.6 Hz, 2H), 2.75 (t, *J* = 8.0 Hz, 4H), 1.73-1.65 (m, 4H), 1.36-1.16 (m, 24H), 0.86 (t, *J* = 4.4 Hz, 6H).

2,6-Didecylpyridine (S24d). Prepared from **S23d** and purified by FCC (petroleum ether:dichloromethane 3:1 to 1:1) which gave the desired product in a yield of (153 mg) 71%. ^{1}H NMR (400MHz, $CDCl_3$): δ 7.48 (t, *J* = 7.6 Hz, 1H), 6.94 (d, *J* = 7.6 Hz, 2H), 2.74 (t, *J* = 8.0 Hz, 4H), 1.73-1.65 (m, 4H), 1.32-1.25 (m, 28H), 0.88 (t, *J* = 6.8 Hz, 6H).

2,6-Didodecylpyridine (S24e). Prepared from **S23e** and purified by FCC (petroleum ether:dichloromethane 4:1 to 1:1) which gave the desired product in a yield of (440 mg) 86%. ^{1}H NMR (400MHz, $CDCl_3$): δ 7.48 (t, *J* = 7.6 Hz, 1H), 6.94 (d, *J* = 7.6 Hz, 2H), 2.75 (t, *J* = 7.6 Hz, 4H), 1.73-1.65 (m, 4H), 1.35-1.25 (m, 36H), 0.88 (t, *J* = 6.8 Hz, 6H).

2,6-Bis((trimethylsilyl)ethynyl)pyridine (S32). 2,6-dibromopyridine (9.00 g, 38.0 mmol), $Pd(PPh_3)_4$ (2.20 g, 1.90 mmol), CuI (361 mg, 1.90 mmol), diisopropylamine (9 mL) and toluene (100 mL) were stirred at r.t. and trimethylsilylacetylene (13.0 mL, 91.2 mmol) was added. The mixture was stirred overnight followed by filtration over Celite using CH_2Cl_2. The filtrate was concentrated under reduced pressure, dissolved in CH_2Cl_2, and washed with an 1M aqueous NH_4Cl solution. The organic layer was dried over $MgSO_4$, filtered and evaporated to dryness. Yield quantitative and used in the next step without further purification. ^{1}H NMR ($CDCl_3$): δ 7.61 (t, *J* = 8.0 Hz, 1H), 7.38 (d, *J* = 7.6 Hz, 2H), 0.25 (s, 18H).

2,6-Bis((4-bromophenyl)ethynyl)pyridine (S33). To a solution of CuCl (346 mg, 3.50 mmol), PPh_3 (918 mg, 3.50 mmol) and potassium benzoate (11.3 g, 70.7 mmol) in 38 mL DMI (1,3-dimethyl-2-imidazolidinone) were added compound **S32** (9.60 g, 35.4 mmol) and 1-bromo-4-iodobenzene (20.0 g, 70.7 mmol) at r.t. The mixture was stirred at 120 °C for 4 h after which full consumption of **S32** was seen. The mixture was cooled down, quenched with a 3M HCl (aq.) solution. The organics were extracted with CH_2Cl_2, and washed with subsequently $NaHCO_3$ and brine. The organic layer was dried over $MgSO_4$, filtered and the solvents were evaporated under vacuum. FCC (petroleum ether:dichloromethane 10:1 to 2:1) gave the desired product. Yield (4.44 g) 29%; ^{1}H NMR ($CDCl_3$): δ 7.70 (t, *J* = 8.0 Hz, 1H), 7.52-7.45 (m, 10H).

General Suzuki reaction procedure yielding compounds S34a-e.

Compound **S33** (0.2 mmol, 1.0 eq.), the respective substituted-phenylboronic acid (0.4 mmol, 2.0 eq.), 2M K_2CO_3 (10 eq.) (aq.) were dissolved in a mixture of 3 mL toluene and 0.4 mL of ethanol. $Pd(PPh_3)_4$ (0.02 mmol, 0.1 eq.) were added and the mixture was heated in the microwave at 100 °C under a nitrogen atmosphere for 24 h. After cooling down to room temperature, EtOAc was added and a precipitate was formed (**S34b-e**). The precipitate was collected by filtration, resulting in the desired products.

2,6-Bis((2'-methylbiphenyl-4-yl)ethynyl)pyridine (S34a). Prepared from 2-methylphenyl boronic acid according to the general procedure, but a precipitate was not formed after addition of EtOAc. The organic layer was washed with a 2 × 0.5 M NaOH solution, dried over $MgSO_4$, filtered and the solvents were evaporated *in vacuo*. Used this as a crude mixture in the next reaction. Yield (37 mg) 50%. ESI-MS: 460.2 $[M+H]^+$.

2,6-Bis((3'-methylbiphenyl-4-yl)ethynyl)pyridine (S34b). Prepared from 3-methylphenyl boronic acid according to the general procedure. Yield (17 mg) 16%; ^{1}H NMR ($CDCl_3$): δ 7.72-7.67 (m, 5H), 7.60 (d, *J* = 8.4 Hz, 4H), 7.50 (d, *J* = 8.0 Hz, 2H), 7.42 (d, J = 8.8 Hz, 4H), 7.35 (t, *J* = 7.2 Hz, 2H), 7.19 (d, *J* = 7.2 Hz, 2H), 2.43 (s, 6H).

2,6-Bis((4'-methylbiphenyl-4-yl)ethynyl)pyridine (S34c) was obtained as a white solid. Yield (13 mg) 18%; ^{1}H NMR ($CDCl_3$): δ 7.72-7.70 (m, 5H), 7.59 (d, *J* = 8.0 Hz, 4H), 7.52-7.49 (m, 6H), 7.30-7.24 (m, H), 2.41 (s, 6H).

2,6-Bis((4'-methoxybiphenyl-4-yl)ethynyl)pyridine (S34d). Prepared from 4-methoxyphenyl-boronic acid according to the general procedure. Yield (55 mg) 49%; ^{1}H NMR ($CDCl_3$): δ 7.72-7.64 (m, 5H), 7.57-7.45 (m, 9H), 7.00 (d, *J* = 8.0 Hz, 4H), 7.30-7.24 (m, H), 2.41 (s, 6H).

2,6-Bis((4'-chlorobiphenyl-4-yl)ethynyl)pyridine (S34e). Prepared from 4-chlorophenyl boronic acid according to the general procedure. Yield (56 mg) 49%; ^{1}H NMR ($CDCl_3$): δ 7.74-7.65 (m, 5H), 7.59-7.47 (m, 10H), 7.43 (d, J = 8.4 Hz, 4H).

4'-Bromo-3-methoxybiphenyl (S43a). Palladium acetate (40.0 mg, 0.18 mmol) was added to mixture of 1-bromo-4-iodobenze (500 mg, 1,77 mmol), 3-methoxy-phenylboronic acid (269 mg, 1.77 mmol), triphenylphosphine (139 mg, 0.53 mmol), a 2M K_2CO_3 aqueous solution (5 mL) in toluene (15 mL) and EtOH (2 mL). This mixture was heated at 50 °C for 24 h., after which it was cooled to room temperature and partitioned between ethyl acetate and water. The organic layer was washed with brine, dried over $MgSO_4$, filtered and evaporated. FCC (petroleum ether:ethyl acetate 1:0 to 4:1) gave the desired product. Yield

(126 mg) 27%; ^{1}H NMR ($CDCl_3$): δ 7.55 (d, J = 8.4 Hz, 2H), 7.45 (d, J = 8.8 Hz, 2H), 7.36 (t, J = 8.0 Hz, 1H), 7.15-7.13 (m, 1H), 7.08 (t, J = 2.4 Hz, 1H), 6.93-6.90 (m, 1H), 3.86 (s, 3H).

4'-Bromo-3-chlorobiphenyl (S43b). Prepared from 1-bromo-4-iodobenzene and 3-chloro-phenylboronic following the procedure of 4-bromo-3-methoxybiphenyl (**S43a**). The reaction was performed at 80° C for 20 h. FCC (petroleum ether) gave the compound 190 mg, 40%. ^{1}H NMR ($CDCl_3$): δ 7.56 (d, J = 8.4 Hz, 2H), 7.53 (t, J = 1.6 Hz, 1H), 7.47-7.43 (m, 3H), 7.36 (t, J = 8.0 Hz, 1H), 7.34-7.31 (m, 1H).

General procedure for Sonogashira coupling between 4'-bromo-3-*substituted*-biphenyl and ethynyltrimethylsilane. Compound **S43a** (126 mg, 0.48 mmol), $PdCl_2(PPh_3)_2$ (7.0 mg, 0.01 mmol), CuI (4.0 mg, 0.02 mmol), PPh_3 (5.0 mg, 0.02 mmol) and trimethylsilylacetylene (123 µL, 0.86 mmol) were dissolved in THF (1 mL) and piperidine (200 µl) was added. This was heated in the microwave at 120 °C for 12 min. The mixture was extracted with diethyl ether and washed with aq. H_2SO_4 (10%), water and brine. The organic layer was dried over $MgSO_4$, filtered and evaporated. FCC (petroleum ether:ethyl acetate 1:0 to 10:1) gave the desired **((3'-Methoxybiphenyl-4-yl)ethynyl)trimethylsilane (S44a).** Yield (104 mg) 78%. ^{1}H NMR ($CDCl_3$): δ 7.53 (s, 4H), 7.35 (t, J = 8.0 Hz, 1H), 7.18-7.15 (m, 1H), 7.12-7.00 (m, 1H), 6.90 (dd, J^1 = 8.0 Hz, J^2 = 2.8 Hz, 1H), 3.86 (s, 3H), 0.27 (s, 9H).

((3'-Chlorobiphenyl-4-yl)ethynyl)trimethylsilane (S44b). Following the procedure of **S44a** starting from **S43b**. Yield (49 mg) 64%.^{1}H NMR ($CDCl_3$): δ 7.56 (t, J = 2.0 Hz, 1H), 7.53 (d, J = 8.4 Hz, 2H), 7.50 (d, J = 8.8 Hz, 2H), 7.45 (dt, J^1 = 7.6 Hz, J^2 = 1.6 Hz, 1H), 7.36 (t, J = 7.6 Hz, 1H), 7.32 (dt, J^1 = 8.0 Hz, J^2 = 2.0 Hz, 1H), 0.27 (s, 9H).

4'-Ethynyl-3-methoxybiphenyl (S45). To a solution of **S44a** (104 mg, 0.37 mmol) in diethyl ether (3 mL) was added methanol (3 mL) and 2M NaOH (1 mL). After 10 min of stirring at room temperature the mixture was neutralized with 2M HCl (aq.). The layers were separated and the organic layer was washed with brine and water, dried, filtered over $MgSO_4$ and concentrated. The product was used without further purification.

2,6-Bis((2'-methoxybiphenyl-4-yl)ethynyl)pyridine (S46). Reaction conditions according to the general Sonogashira coupling procedure (**S23a-e**), starting from **S45** and **S21**. Purified by FCC (petroleum ether:ethyl acetate 4:1 to 1:1). Yield (23 mg) 25%. ^{1}H NMR ($CDCl_3$): δ 7.72-7.65 (m, 5H), 7.60 (d, J = 8.4 Hz, 4H), 7.51 (d, J = 7.6 Hz, 2H), 7.38 (t, J = 8.4 Hz, 2H), 7.20 (d, J = 8.0 Hz, 2H), 7.14 (s, 2H), 6.93 (dd, J^1 = 8.2 Hz, J^2 = 2.0 Hz, 2H), 3.88 (s, 6H).

2,6-Bis((2'-chlorobiphenyl-4-yl)ethynyl)pyridine (S47). Starting from

compounds **S21** and **S44b**. FCC (petroleum ether:dichloromethane 20:1 to 1:2). Yield (16 mg) 19%. ^{1}H NMR ($CDCl_3$): δ 7.70-7.66 (m, 4H), 7.59-7.55 (m, 6H), 7.53 (d, *J* = 5.2 Hz, 1H), 7.50-7.44 (m, 4H), 7.39 (t, *J* = 8.0 Hz, 2H), 7.34 (d, *J* = 8.0 Hz, 2H).

***N*-Ethyl-*N*-(3-(*p*-tolyl)prop-2-yn-1-yl)heptan-1-amine (19).** To a solution of **S14** (300 mg, 1 mmol) in DMF (5 mL) was added K_2CO_3 (415 mg, 3 mmol) followed by *N*-ethylheptylamine (280 µL, 1.5 mmol). The mixture was stirred at r.t. for 1 hour and diluted with water (5 mL), extracted with EtOAc (3 × 10 mL) and the organic layers were dried on $MgSO_4$, filtered and the solvent was removed *in vacuo*. The crude residue was purified by flash chromatography on silica gel (20% EtOAc-Petroleum ether) to afford pure **19** as an oil. Yield (228 mg) 84%; ^{1}H NMR (400 MHz, $CDCl_3$) δ 7.32 (d, *J* = 8.0 Hz, 2H), 7.10 (d, *J* = 8.0 Hz, 2H), 3.62 (s, 2H), 2.61 (q, *J* = 7.2 Hz, 2H), 2.53 (t, *J* = 7.6 Hz, 2H), 2.34 (s, 3H), 1.52–1.49 (m, 2H), 1.31–1.26 (m, 8H), 1.11 (t, *J* = 7.2 Hz, 3H), 0.88 (t, *J* = 7.2 Hz, 3H) ppm; ^{13}C NMR (101 MHz, $CDCl_3$) δ 137.9, 131.6, 129.0, 120.3, 85.0, 83.8, 53.6, 47.7, 42.1, 31.9, 29.3, 27.6, 27.5, 22.7, 21.4, 14.1, 12.7 ppm. HPLC: t_R = 7.39 min; HRMS (ESI): *m/z* $[M + H]^+$ calcd for $C_{19}H_{29}N$: 272.2373, found: 272.2370.

***N*-Ethyl-*N*-propyl-3-(*p*-tolyl)prop-2-yn-1-amine (20).** To a solution of **S14** (300 mg, 1 mmol) in DMF (5 mL) was added K_2CO_3 (415 mg, 3 mmol) followed by *N*-ethylpropylamine (180 µL, 1.5 mmol). The mixture was stirred at r.t. for 1 hour and diluted with water (5 mL), extracted with EtOAc (3 × 10 mL) and the organic layers were dried on $MgSO_4$, filtered and the solvent was removed *in vacuo*. The crude residue was purified by flash chromatography on silica gel (20% EtOAc- Petroleum ether) to afford pure **20** as oil. Yield (170 mg) 79%; ^{1}H NMR (400 MHz, $CDCl_3$) δ 7.32 (d, *J* = 8.0 Hz, 2H), 7.10 (d, *J* = 8.0 Hz, 2H), 3.62 (s, 2H), 2.61 (q, *J* = 7.2 Hz, 2H), 2.50 (t, *J* = 7.6 Hz, 2H), 2.34 (s, 3H), 1.53 (sex, *J* = 7.6 Hz, 2H), 1.11 (t, *J* = 7.2 Hz, 3H), 0.93 (t, *J* = 7.6 Hz, 3H) ppm; ^{13}C NMR (101 MHz, $CDCl_3$) δ 137.9, 131.6, 129.0, 120.3, 85.0, 83.8, 55.6, 47.6, 42.1, 21.4, 20.8, 12.7, 12.0 ppm. HPLC: t_R = 5.70 min; HRMS (ESI): *m/z* $[M + H]^+$ calcd for $C_{15}H_{21}$: 216.1747, found: 216.1745.

General methylation procedure to yield pyridines 24, 25, 27-30, 39-44 and 46.

The respective compound **S23e, S24a-e, S34a-e, S46** and **S47** (1.0 eq.) was dissolved in CH_2Cl_2 (40 mL per mmol) and stirred at 0 °C under a N_2 atmosphere. Methyl trifluoromethanesulfonate (2.8 eq.) was added and the mixture was stirred overnight. After adsorption of the crude on silica, FCC gave the desired compound eluting with a mixture of dichloromethane:methanol.

2,6-Dihexyl-1-methylpyridinium trifluoromethanesulfonate (24). Prepared from **S24a** and purified by FCC (dichloromethane:methanol 60:1 to 20:1) to give the desired product. Yield (660 mg) 85%; ^{1}H NMR (400MHz, $CDCl_3$): δ 8.20 (t, *J* = 8.0 Hz, 1H), 7.64 (d, *J* = 8.0 Hz, 2H), 4.21 (s, 3H), 3.12 (t, *J* = 7.6 Hz, 4H), 1.81-1.74 (m, 4H),), 1.52-1.45 (m, 4H), 1.39-1.29 (m, 8H), 0.91 (t, *J* = 6.8 Hz, 6H); ^{13}C NMR (101 MHz, $CDCl_3$): δ 159.7, 144.2, 126.0, 39.7, 34.5, 31.4, 28.9, 27.6, 22.5, 14.1 ppm. HPLC purity: 99.3% (t_R 8.24 min); ESI-MS: 262.27 [M].

2,6-Diheptyl-1-methylpyridinium trifluoromethanesulfonate (25). Prepared from **S24b** and purified by FCC (dichloromethane:methanol 30:1 to 20:1) to give the desired product. Yield (143 mg) 86%; ^{1}H NMR (400MHz, $CDCl_3$): δ 8.18 (t, *J* = 7.6 Hz, 1H), 7.63 (d, *J* = 8.0 Hz, d), 4.22 (s, 3H), 3.13 (t, *J* = 8.0 Hz, 4H), 1.82-1.74 (m, 4H), 1.52-1.44 (m, 4H), 1.41-1.36 (m, 12H), 0.90 (t, *J* = 6.4 Hz, 6H); ^{13}C NMR (101 MHz, $CDCl_3$): δ 159.8, 144.1, 126.0, 122.4, 119.2, 39.7, 34.6, 31.7, 29.3, 29.0, 27.7, 22.7, 14.2 ppm. HPLC purity: 97% (t_R 8.96 min); ESI-MS: 290.33 [M].

2,6-Dinonyl-1-methylpyridinium trifluoromethanesulfonate (27). Prepared from **S24c** and purified by FCC (dichloromethane:methanol 30:1 to 15:1) to give the desired product. Yield (87 mg) 65%; ^{1}H NMR (400MHz, $CDCl_3$): δ 8.18 (t, *J* = 8.0 Hz, 1H), 7.63 (d, *J* = 8.0 Hz, 2H), 4.22 (s, 3H), 3.12 (t, *J* = 7.6 Hz, 4H), 1.82-1.74 (m, 4H), 1.50-1.46 (m, 4H), 1.44-1.28 (m, 20H), 0.89 (t, *J* = 6.4 Hz, 6H); ^{13}C NMR (101 MHz, $CDCl_3$): δ 159.9, 144.0, 126.0, 39.8, 34.6, 32.0, 29.5, 29.4, 27.7, 22.8, 14.2 ppm. HPLC purity: 100% (t_R 10.21 min); ESI-MS: 346.40 [M].

2,6-Didecyl-1-methylpyridinium trifluoromethanesulfonate (28). Prepared from **S24d** and purified by FCC (dichloromethane:methanol 60:1 to 10:1) to give the desired product. Yield (166 mg) 74%; ^{1}H NMR (400MHz, $CDCl_3$): δ 8.18 (t, *J* = 8.0 Hz, 1H), 7.63 (d, *J* = 8.0 Hz, 2H), 4.22 (s, 3H), 3.13 (t, *J* = 8.0 Hz, 4H), 1.82-1.74 (m, 4H), 1.50-1.44 (m, 4H), 1.39-1.28 (m, 24H), 0.89 (t, *J* = 6.8 Hz, 6H); ^{13}C NMR (101 MHz, $CDCl_3$): δ 159.7, 144.0, 125.9, 39.6, 34.4, 31.9, 29.5, 29.4, 29.3, 29.2, 27.6, 22.7, 14.1 ppm. HPLC purity: 100% (t_R 10.77 min); ESI-MS: 374.40 [M].

2,6-Didodecyl-1-methylpyridinium trifluoromethanesulfonate (29). Prepared from **S24e** and purified by FCC (dichloromethane:methanol 30:1 to 20:1) to give the desired product. Yield (536 mg) 87%; ^{1}H NMR (400MHz, $CDCl_3$): δ 8.19 (t, *J* = 8.0 Hz, 1H), 7.63 (d, *J* = 7.6 Hz, 2H), 4.21 (s, 3H), 3.12 (t, *J* = 8.0 Hz, 4H), 1.81-1.73 (m, 4H), 1.51-1.44 (m, 4H), 1.38-1.27 (m, 32H), 0.88 (t, *J* = 6.8 Hz, 6H); ^{13}C NMR (101 MHz, $CDCl_3$): δ 159.8, 144.1, 126.0, 39.7, 34.6, 32.0, 29.8, 29.7, 29.7, 29.6, 29.5, 29.4, 29.3, 27.7, 22.8, 14.2 ppm. HPLC purity: 100%

(t_R 11.84 min); ESI-MS: 430.53 [M].

2,6-Di(dodec-1-ynyl)-1-methylpyridinium trifluoromethanesulfonate (30). Prepared from **S23e** and purified by FCC (dichloromethane:methanol 40:1 to 20:1) to give the desired product. Yield (675 mg) 94%; ^{1}H NMR (400MHz, $CDCl_3$): δ 8.38 (t, *J* = 8.0 Hz, 1H), 7.90 (d, *J* = 8.0 Hz, 2H), 4.49 (s, 3H), 2.65 (t, *J* = 7.2 Hz, 4H), 1.74-1.65 (m, 4H), 1.48-1.41 (m, 4H), 1.30-1.27 (m, 24H), 0.88 (t, *J* = 6.8 Hz, 6H); ^{13}C NMR (101 MHz, $CDCl_3$): δ 144.3, 139.5, 130.7, 112.8, 72.9, 45.1, 32.0, 29.7, 29.5, 29.4, 29.2, 29.1, 27.6, 22.9, 20.3, 14.2 ppm. HPLC purity: 100% (t_R 11.57 min); ESI-MS: 422.40 [M].

2,6-Di([4-(2-methylphenyl)phenyl]ethynyl)-1-methylpyridinium trifluoromethanesulfonate (39). Prepared from **S34a** and purified by FCC (dichloromethane:methanol 30:1 to 20:1) and preparative HPLC to give the desired product. Yield (1 mg) 96%; ^{1}H NMR (400MHz, $CDCl_3$): δ 8.47 (t, *J* = 8.0 Hz, 1H), 8.10 (d, *J* = 8.0 Hz, 2H), 7.77 (d, *J* = 8.0 Hz, 4H), 7.46 (d, *J* = 8.0 Hz, 4H), 7.31-7.09 (m, 8H), 4.74 (s, 3H), 2.30 (s, 6H). HPLC purity: 96% (t_R 9.97 min); ESI-MS: 474.33 [M].

2,6-Di([4-(3-methylphenyl)phenyl]ethynyl)-1-methylpyridinium trifluoromethanesulfonate (40). Prepared from **S34b** and purified by FCC (dichloromethane:methanol 30:1 to 20:1) to give the desired product. Yield (18 mg) 78%. ^{1}H NMR (400MHz, $CDCl_3$): δ 8.40 (t, *J* = 8.0 Hz, 1H), 8.03 (d, *J* = 8.0 Hz, 2H), 7.73 (d, *J* = 8.0 Hz, 4H), 7.65 (d, *J* = 8.0 Hz, 4H), 7.41-7.37 (m, 4H), 7.35 (t, *J* = 7.6 Hz, 2H), 7.22 (d, *J* = 7.2 Hz, 2H), 4.65 (s, 3H), 2.41 (s, 6H); ^{13}C NMR (101 MHz, $CDCl_3$): δ 145.0, 143.9, 139.5, 138.9, 133.5, 129.4, 129.1, 128.1, 127.7, 124.4, 117.5, 109.0, 81.2, 45.5, 21.7 ppm. HPLC purity: 98.65% (t_R 10.24 min); ESI-MS: 474.33 [M].

2,6-Di([4-(3-methoxyphenyl)phenyl]ethynyl)-1-methylpyridinium trifluoromethanesulfonate (41). Prepared from **S46** and purified by FCC (dichloromethane:methanol 20:1 to 10:1) to give the desired product. Yield (12 mg) 36%; ^{1}H NMR (400MHz, $CDCl_3$): δ 8.39 (t, *J* = 8.0 Hz, 1H), 8.02 (d, *J* = 8.0 Hz, 2H), 7.73 (d, *J* = 8.0 Hz, 4H), 7.65 (d, J = 8.4 Hz, 4H), 7.37 (t, *J* = 7.6 Hz, 2H), 7.18 (d, *J* = 8.0 Hz, 2H), 7.11 (s, 2H), 6.94 (dd, J^1 = 8.2 Hz, J^2 = 2.0 Hz, 2H), 4.63 (s, 3H), 3.86 (s, 6H); ^{13}C NMR (101 MHz, $CDCl_3$): δ 160.3, 144.6, 143.9, 140.9, 139.3, 133.5, 130.8, 130.3, 127.7, 119.7, 117.7, 114.0, 113.0, 108.8, 81.3, 77.4, 55.5, 45.5, 29.9 ppm. HPLC purity: 99% (t_R 9.56 min); ESI-MS: 506.33 [M].

2,6-Di([4-(3-chlorophenyl)phenyl]ethynyl)-1-methylpyridinium trifluoromethanesulfonate (42). Prepared from **S47** and purified by FCC (dichloromethane:methanol 20:1 to 10:1) to give the desired product. Yield (9 mg) 45%; ^{1}H NMR (400MHz, $CDCl_3$): δ ^{1}H NMR (400 MHz, $CDCl_3$): δ 8.43 (t, *J* = 8.0 Hz, 1H), 8.08 (d, *J* = 8.0 Hz, 2H), 7.78 (d, *J* = 8.0 Hz, 4H), 7.65 (d, *J* = 8.0 Hz, 4H),

7.57 (s, 2H), 7.48 (d, *J* = 7.2 Hz, 2H), 7.42-7.37 (m, 4H), 4.70 (s, 3H); ^{13}C NMR (101 MHz, $CDCl_3$/MeOD): δ 143.8, 143.4, 141.0, 139.3, 134.9, 133.3, 130.7, 130.3, 128.5, 127.6, 127.1, 125.3, 117.9, 108.5, 80.8, 45.0, 29.5 ppm. HPLC purity: 99% (t_R 10.20 min); ESI-MS: 514.33 [M].

2,6-Di(4-(4-methylphenyl)phenylethynyl)-1-methylpyridinium trifluoromethanesulfonate (43). Prepared from **S34c** and purified by FCC (dichloromethane:methanol 30:1 to 5:1) to give the desired product. Yield (27 mg) 48%; ^{1}H NMR (400MHz, $CDCl_3$): δ 8.43 (t, *J* = 8.0 Hz, 1H), 8.06 (d, *J* = 8.0 Hz, 2H), 7.75 (d, *J* = 8.4 Hz, 4H), 7.67 (d, *J* = 8.4 Hz, 4H), 7.52 (d, *J* = 8.0 Hz, 4H), 7.29-7.26 (m, 4H), 4.68 (s, 3H), 2.41 (s, 6H); ^{13}C NMR (101 MHz, $CDCl_3$/MeOD): δ 144.9, 143.9, 139.4, 138.8, 136.3, 133.4, 133.3, 130.6, 129.8, 127.4, 127.0, 117.0, 109.1, 80.9, 77.3, 21.1 ppm. HPLC purity: 99% (t_R 10.28 min); ESI-MS: 474.40 [M].

2,6-Di([4-(4-methoxyphenyl)phenyl]ethynyl)-1-methylpyridinium trifluoromethanesulfonate (44). Prepared from **S34d** and purified by FCC (dichloromethane:methanol 30:1 to 10:1) to give the desired product. Yield (42 mg) 58%; ^{1}H NMR (400MHz, $CDCl_3$): δ 8.42 (t, *J* = 8.0 Hz, 1H), 8.04 (d, *J* = 8.0 Hz, 2H), 7.73 (d, *J* = 8.4 Hz, 4H), 7.65 (d, *J* = 8.4 Hz, 4H), 7.57 (d, *J* = 8.8 Hz, 4H), 7.00 (d, *J* = 8.8 Hz, 4H), 4.67 (s, 3H), 3.86 (s, 6H); ^{13}C NMR (101 MHz, $CDCl_3$/MeOD): δ 160.1, 144.5, 143.7, 139.3, 133.3, 131.6, 130.4, 128.3, 127.0, 116.5, 114.5, 109.3, 80.7, 55.4, 44.9 ppm. HPLC purity: 100% (t_R 9.78 min); ESI-MS: 506.33 [M].

2,6-Di([4-(4-hydroxyphenyl)phenyl]ethynyl)-1-methylpyridinium trifluoromethanesulfonate (45). 44 (27 mg, 0.04 mmol) was dissolved in 2 mL CH_2Cl_2 and cooled to -78 °C under a nitrogen atmosphere. An 1M solution of BBr_3 in CH_2Cl_2 (0.4 mL) was added and the reaction mixture was allowed to warm up to room temperature and stirring was continued for 2 h at room temperature, after which as shown by TLC (dichloromethane:methanol 30:1) full conversion was reached. The reaction mixture was re cooled to -78 °C and quenched with H_2O. After an hour the precipitate was filtered off and washed with H_2O and CH_2Cl_2 respectively and dried *in vacuo*. Yield (12 mg) 48%. ^{1}H NMR (400MHz, DMSO): δ 9.81 (s, 2H), 8.56 (t, *J* = 8.4 Hz, 1H), 8.36 (d, *J* = 7.6 Hz, 2H), 7.89 (d, *J* = 8.0 Hz, 4H), 7.83 (d, *J* = 8.4 Hz, 4H), 7.64 (d, *J* = 8.4 Hz, 4H), 6.90 (d, *J* = 8.8 Hz, 4H), 4.58 (s, 3H); ^{13}C NMR (151 MHz, DMSO): δ 158.2, 143.6, 143.2, 133.3, 130.6, 129.1, 128.2, 126.3, 116.4, 115.9, 106.0, 81.7, 45.2 ppm. HPLC purity 99% (t_R 8.38 min); ESI-MS: 478.33 [M].

2,6-Di([4-(4-chlorophenyl)phenyl]ethynyl)-1-methylpyridinium trifluoromethanesulfonate (46). Prepared from **S34e** and purified by FCC (dichloromethane:methanol 30:1 to 10:1) to give the desired product. Yield (42 mg) 58%; ^{1}H NMR (400MHz, $CDCl_3$): δ 8.43 (t, *J* = 8.0 Hz, 1H), 8.08 (d, *J* = 8.4 Hz, 2H),

7.79 (d, J = 8.4 Hz, 4H), 7.67 (d, J = 8.4 Hz, 4H), 7.56 (d, J = 8.4 Hz, 4H), 7.46 (d, J = 8.4 Hz, 4H), 4.74 (s, 3H); ^{13}C NMR (101 MHz, $CDCl_3$/MeOD): δ 143.8, 143.6, 139.3, 137.7, 134.8, 133.4, 130.6, 129.2, 128.4, 127.4, 117.6, 108.6, 80.9, 45.0 ppm. HPLC purity: 99% (t_R 10.39 min); ESI-MS: 514.27 [M].

Biology

Chemical and regents

[^{3}H]Dofetilide (specific activity 82.3 Ci·mmol^{-1}) was purchased from Perkin-Elmer (Groningen, The Netherlands). Astemizole was purchased from Sigma Aldrich (Zwijndrecht, The Netherlands). Bovine serum albumin (BSA, fraction V) was purchased from Sigma (St. Louis, MO, USA). G418 was obtained from Stratagene (Cedar Creek, USA). All the other chemicals were of analytical grade and purchased from standard commercial sources. Human embryonic kidney cells stably expressing the K_v11.1 channel (HEK293K_v11.1) were kindly provided by Dr Eckhard Ficker (University of Cleveland, USA).

Cell culture and membrane preparation

HEK293K_v11.1 cells were cultured and membranes were prepared and stored as described previously.[51]

Radioligand displacement assay

The binding affinity of all tested compounds was evaluated at 25 ºC in a [^{3}H] dofetilide competitive displacement assay as reported earlier.[2]

Radioligand competition association assay

The binding kinetics of unlabeled compounds were determined at 25 ºC using a [^{3}H]dofetilide competition association assay as described before,[2] and the concentrations of unlabeled compounds used in this assay were equivalent to their IC_{50} values.

Patch clamp assay

HEK293K_v11.1 cells were cultured on 10 mm glass coverslips and placed in a perfusion chamber (Cell Microcontrols, Norfolk, USA) at room temperature and perfused with control or test solutions. Whole cell patch clamp measurements and data acquisition were performed using an Axopatch-200B amplifier controlled by

the pClamp software package version 10 (Axon Instruments, Foster City, CA). Patch pipettes were made with a Sutter P-2000 micropipette puller (Sutter Instrument Company, Novato, USA) and had resistances of 1.5-2.5 MΩ after having been fire polished and filled with pipette solution. Control bath perfusion solution contained (mM): 140 NaCl, 4 KCl, 10 HEPES, 2 $CaCl_2$, 1 $MgCl_2$ (pH 7.2, NaOH), and the pipette filling solution consisted of (mM): 10 KCl, 125 K-Gluconate, 0.6 $CaCl_2$, 2 $MgCl_2$, 5 HEPES, 4 Na_2ATP, 5 EGTA (pH 7.2, KOH). After establishing the whole cell configuration, capacitive transients and pipette access resistance were compensated for by 80%.

The pulse protocol for whole cell voltage clamp measurements of K_v11.1-mediated ion currents was as following. Cells were depolarized to 20 mV from a holding potential -80 mV for 4000 ms, allowing a step current due to activation and inactivation of the K_v11.1 channels. This was followed by repolarization to a test potential of -50 mV for 5000 ms, during which a tail current was induced by the fast recovery from inactivation and slow deactivation of the channels. The peak tail currents were used for data analysis, and current inhibition was derived from dividing the mean tail current in the presence of selected compounds by the mean tail current under control conditions. Concentration-dependent effects of compounds **21** and **38** on K_v11.1 currents were tested at five different concentrations with an equilibrium time of 6.5 min for each concentration in a perfusion system. To determine time-dependent effects, wash-in experiments were performed with a perfusion of bath solution containing 1 µM **21** or **38**. Clampfit 10.4 (Axon Instruments, Foster City, CA) and Prism v. 5.1 (GraphPad, San Diego, CA, USA) were used in analyzing, processing and plotting the data.

Data analysis

All experimental data were analyzed using the non-linear regression curve fitting program Prism v. 5.1 (GraphPad, San Diego, CA, USA). Apparent inhibitory binding constants (K_i values) were derived from the IC_{50} values according to the Cheng-Prusoff equation with the K_D value obtained from saturation assay.[2, 35] Association and dissociation rates for unlabeled compounds were calculated by fitting the data into the competition association model using "kinetics of competitive binding":[34]

$$K_A = k_1[L] + k_2$$

$$K_B = k_3[I] + k_4$$

$$S = \sqrt{(K_A - K_B)^2 + 4k_1k_3LI10^{-18}}$$

$$K_F = 0.5\ (K_A + K_B + S)$$

$$K_S = 0.5\ (K_A + K_B - S)$$

$$Q = \frac{B_{max} k_1 L 10^{-9}}{K_F - K_S}$$

$$Y = Q\left(\frac{k_4(K_F - K_S)}{K_F K_S} + \frac{k_4 - K_F}{K_F} e^{(-K_F X)} - \frac{k_4 - K_S}{K_S} e^{(-K_S X)}\right)$$

Where X is the time (min), Y the specific binding of [^{3}H]dofetilide, k_1 and k_2 are the k_{on} ($M^{-1}\cdot min^{-1}$) and k_{off} (min^{-1}) of [^{3}H]dofetilide, L the concentration of [^{3}H]dofetilide (nM), B_{max} the maximum specific binding (dpm) and I the concentration of the unlabelled compound (nM). Fixing these parameters allowed the following parameters to be calculated: k_3, which is the k_{on} value ($M^{-1}\cdot min^{-1}$) of the unlabelled compound and k_4, which is the k_{off} value (min^{-1}) of the unlabelled compound. The association and dissociation rates were used to calculate the kinetic K_D values from the following equation: $K_D = k_{off}/k_{on}$. The residence time (RT) was calculated according to the formula: $RT = 1/k_{off}$. All values in this study are means of at least three independent experiments with SEM.

References

1. Heijman, J.; Voigt, N.; Carlsson, L. G.; Dobrev, D. Cardiac safety assays. *Curr. Opin. Pharmacol.* **2014,** *15*, 16-21.

2. Yu, Z.; IJzerman, A. P.; Heitman, L. H. K_v11.1 (hERG)-induced cardiotoxicity: A molecular insight from a binding kinetics study of prototypic K_v11.1 (hERG) inhibitors. *Br. J. Pharmacol.* **2015,** *172*, 940-945.

3. Sanguinetti, M. C.; Tristani-Firouzi, M. hERG potassium channels and cardiac arrhythmia. *Nature* **2006,** *440*, 463-469.

4. Vandenberg, J. I.; Perry, M. D.; Perrin, M. J.; Mann, S. A.; Ke, Y.; Hill, A. P. hERG K^+ channels: Structure, function, and clinical significance. *Physiol. Rev.* **2012,** *92*, 1393-1478.

5. Townsend, C. Is there a need to add another dimension (time) to the evaluation of the arrhythmogenic potential of new drug candidates *in vitro*? *Circulation* **2014,** *130*, 219-220.

6. Hill, A. P.; Perrin, M. J.; Heide, J.; Campbell, T. J.; Mann, S. A.; Vandenberg, J. I. Kinetics of drug interaction with the K_v11.1 potassium channel. *Mol. Pharmacol.* **2014,** *85*, 769-776.

7. Redfern, W. S.; Carlsson, L.; Davis, A. S.; Lynch, W. G.; MacKenzie, I.; Palethorpe, S.; Siegl, P. K. S.; Strang, I.; Sullivan, A. T.; Wallis, R.; Camm, A. J.; Hammond, T. G. Relationships between preclinical cardiac electrophysiology, clinical QT interval prolongation and torsade de pointes for a broad range of drugs: Evidence for a provisional safety

margin in drug development. *Cardiovasc. Res.* **2003,** *58*, 32-45.

8. Di Veroli, G. Y.; Davies, M. R.; Zhang, H.; Abi-Gerges, N.; Boyett, M. R. High-throughput screening of drug-binding dynamics to hERG improves early drug safety assessment. *Am. J. Physiol. Heart Circ. Physiol.* **2013,** *304*, H104-H117.

9. Di Veroli, G. Y.; Davies, M. R.; Zhang, H.; Abi-Gerges, N.; Boyett, M. R. hERG inhibitors with similar potency but different binding kinetics do not pose the same proarrhythmic risk: Implications for drug safety assessment. *J. Cardiovasc. Electrophysiol.* **2014,** *25*, 197-207.

10. Ridley, J. M.; Milnes, J. T.; Duncan, R. S.; McPate, M. J.; James, A. F.; Witchel, H. J.; Hancox, J. C. Inhibition of the hERG K^+ channel by the antifungal drug ketoconazole depends on channel gating and involves the S6 residue F656. *FEBS Lett.* **2006,** *580*, 1999-2005.

11. Schneider, E. V.; Bottcher, J.; Huber, R.; Maskos, K.; Neumann, L. Structure-kinetic relationship study of CDK8/CycC specific compounds. *Proc. Natl. Acad. Sci. U.S.A.* **2013,** *110*, 8081-8086.

12. Markgren, P.-O.; Schaal, W.; Hämäläinen, M.; Karlén, A.; Hallberg, A.; Samuelsson, B.; Danielson, U. H. Relationships between structure and interaction kinetics for HIV-1 protease inhibitors. *J. Med. Chem.* **2002,** *45*, 5430-5439.

13. Tummino, P. J.; Copeland, R. A. Residence time of receptor-ligand complexes and its effect on biological function. *Biochemistry* **2008,** *47*, 5481-5492.

14. Goyal, M.; Rizzo, M.; Schumacher, F.; Wong, C. F. Beyond thermodynamics: Drug binding kinetics could influence epidermal growth factor signaling. *J. Med. Chem.* **2009,** *52*, 5582-5585.

15. Vilums, M.; Zweemer, A. J. M.; Yu, Z.; de Vries, H.; Hillger, J. M.; Wapenaar, H.; Bollen, I. A. E.; Barmare, F.; Gross, R.; Clemens, J.; Krenitsky, P.; Brussee, J.; Stamos, D.; Saunders, J.; Heitman, L. H.; IJzerman, A. P. Structure-kinetic relationships-an overlooked parameter in hit-to-lead optimization: A case of cyclopentylamines as chemokine receptor 2 antagonists. *J. Med. Chem.* **2013,** *56*, 7706-7714.

16. Guo, D.; Xia, L.; van Veldhoven, J. P.; Hazeu, M.; Mocking, T.; Brussee, J.; IJzerman, A. P.; Heitman, L. H. Binding kinetics of ZM241385 derivatives at the human adenosine A_{2A} receptor. *ChemMedChem* **2014,** *9*, 752-761.

17. Winquist, J.; Geschwindner, S.; Xue, Y.; Gustavsson, L.; Musil, D.; Deinum, J.; Danielson, U. H. Identification of structural-kinetic and structural-thermodynamic relationships for thrombin inhibitors. *Biochemistry* **2013,** *52*, 613-626.

18. Sager, P. T.; Gintant, G.; Turner, J. R.; Pettit, S.; Stockbridge, N. Rechanneling the cardiac proarrhythmia safety paradigm: A meeting report from the cardiac safety research consortium. *Am. Heart J.* **2014,** *167*, 292-300.

19. Cavero, I.; Holzgrefe, H. Comprehensive *in vitro* proarrhythmia assay, a novel *in vitro/in silico* paradigm to detect ventricular proarrhythmic liability: A visionary 21st cen-

tury initiative. *Expert Opin. Drug Saf.* **2014,** *13*, 745-758.
20. Windisch, A.; Timin, E.; Schwarz, T.; Stork-Riedler, D.; Erker, T.; Ecker, G.; Hering, S. Trapping and dissociation of propafenone derivatives in hERG channels. *Br. J. Pharmacol.* **2011,** *162*, 1542-1552.
21. Linder, T.; Saxena, P.; Timin, E. N.; Hering, S.; Stary-Weinzinger, A. Structural insights into trapping and dissociation of small molecules in K^+ channels. *J. Chem. Inf. Model.* **2014,** *54*, 3218-3228.
22. Shagufta; Guo, D.; Klaasse, E.; de Vries, H.; Brussee, J.; Nalos, L.; Rook, M. B.; Vos, M. A.; van der Heyden, M. A.; IJzerman, A. P. Exploring chemical substructures essential for hERG K^+ channel blockade by synthesis and biological evaluation of dofetilide analogues. *ChemMedChem* **2009,** *4*, 1722-1732.
23. Vilums, M.; Overman, J.; Klaasse, E.; Scheel, O.; Brussee, J.; IJzerman, A. P. Understanding of molecular substructures that contribute to hERG K^+ channel blockade: Synthesis and biological evaluation of E-4031 analogues. *ChemMedChem* **2012,** *7*, 107-113.
24. Louvel, J.; Carvalho, J. F.; Yu, Z.; Soethoudt, M.; Lenselink, E. B.; Klaasse, E.; Brussee, J.; IJzerman, A. P. Removal of human ether-à-go-go related gene (hERG) K^+ channel affinity through rigidity: A case of clofilium analogues. *J. Med. Chem.* **2013,** *56*, 9427-9440.
25. Carvalho, J. o. F.; Louvel, J.; Doornbos, M. L.; Klaasse, E.; Yu, Z.; Brussee, J.; IJzerman, A. P. Strategies to reduce hERG K^+ channel blockade. Exploring heteroaromaticity and rigidity in novel pyridine analogues of dofetilide. *J. Med. Chem.* **2013,** *56*, 2828-2840.
26. Suessbrich, H.; Waldegger, S.; Lang, F.; Busch, A. E. Blockade of hERG channels expressed in xenopus oocytes by the histamine receptor antagonists terfenadine and astemizole. *FEBS Lett.* **1996,** *385*, 77-80.
27. Fitzgerald, P. T.; Ackerman, M. J. Drug-induced Torsades de Pointes: The evolving role of pharmacogenetics. *Heart Rhythm* **2005,** *2*, S30-S37.
28. Rajamani, S.; Shryock, J. C.; Belardinelli, L. Rapid kinetic interactions of ranolazine with hERG K^+ current. *J. Cardiovasc. Pharmacol.* **2008,** *51*, 581-589.
29. Orita, A.; Nakano, T.; An, D. L.; Tanikawa, K.; Wakamatsu, K.; Otera, J. Metal-assisted assembly of pyridine-containing arylene ethynylene strands to enantiopure double helicates. *J. Am. Chem. Soc.* **2004,** *126*, 10389-10396.
30. Nishihara, Y.; Noyori, S.; Okamoto, T.; Suetsugu, M.; Iwasaki, M. Copper-catalyzed Sila-Sonogashira-Hagihara cross-coupling reactions of alkynylsilanes with aryl iodides under palladium-free conditions. *Chem. Lett.* **2011,** *40*, 972-974.
31. Siemsen, P.; Livingston, R. C.; Diederich, F. Acetylenic coupling: A powerful tool in molecular construction. *Angew. Chem. Int. Ed. Engl.* **2000,** *39*, 2632-2657.
32. Shen, X.; Ho, D. M.; Pascal, R. A. Synthesis of polyphenylene dendrimers related to "cubic graphite". *J. Am. Chem. Soc.* **2004,** *126*, 5798-5805.

33. Aggarwal, A. V.; Jester, S. S.; Taheri, S. M.; Foerster, S.; Hoeger, S. Molecular spoked wheels: Synthesis and self-assembly studies on rigid nanoscale 2D objects. *Chem. Eur. J.* **2013,** *19*, 4480-4495.
34. Motulsky, H. J.; Mahan, L. The kinetics of competitive radioligand binding predicted by the law of mass action. *Mol. Pharmacol.* **1984,** *25*, 1-9.
35. Cheng, Y.; Prusoff, W. H. Relationship between the inhibition constant (K_I) and the concentration of inhibitor which causes 50 percent inhibition (I_{50}) of an enzymatic reaction. *Biochem. Pharmacol.* **1973,** *22*, 3099-3108.
36. Jamieson, C.; Moir, E. M.; Rankovic, Z.; Wishart, G. Medicinal chemistry of hERG optimizations: Highlights and hang-ups. *J. Med. Chem.* **2006,** *49*, 5029-5046.
37. Fernandez, D.; Ghanta, A.; Kauffman, G. W.; Sanguinetti, M. C. Physicochemical features of the hERG channel drug binding site. *J. Biol. Chem.* **2004,** *279*, 10120-10127.
38. Zhu, B.; Jia, Z. J.; Zhang, P.; Su, T.; Huang, W.; Goldman, E.; Tumas, D.; Kadambi, V.; Eddy, P.; Sinha, U.; Scarborough, R. M.; Song, Y. Inhibitory effect of carboxylic acid group on hERG binding. *Bioorg. Med. Chem. Lett.* **2006,** *16*, 5507-5512.
39. CCavalli, A.; Buonfiglio, R.; Ianni, C.; Masetti, M.; Ceccarini, L.; Caves, R.; Chang, M. W. Y.; Mitcheson, J. S.; Roberti, M.; Recanatini, M. Computational design and discovery of "minimally structured" hERG blockers. *J. Med. Chem.* **2012,** *55*, 4010-4014.
40. Mitcheson, J. S.; Chen, J.; Lin, M.; Culberson, C.; Sanguinetti, M. C. A structural basis for drug-induced long QT syndrome. *Proc. Natl. Acad. Sci. U.S.A.* **2000,** *97*, 12329-12333.
41. Czodrowski, P. hERG me out. *J. Chem. Inf. Model.* **2013,** *53*, 2240-2251.
42. Pearlstein, R. A.; Vaz, R. J.; Kang, J.; Chen, X.; Preobrazhenskaya, M.; Shchekotikhin, A. E.; Korolev, A. M.; Lysenkova, L. N.; Miroshnikova, O. V.; Hendrix, J.; Rampe, D. Characterization of hERG potassium channel inhibition using CoMSiA 3D QSAR and homology modeling approaches. *Bioorg. Med. Chem. Lett.* **2003,** *13*, 1829-1835.
43. Kramer, C.; Beck, B.; Kriegl, J. M.; Clark, T. A composite model for hERG blockade. *ChemMedChem* **2008,** *3*, 254-265.
44. Farid, R.; Day, T.; Friesner, R. A.; Pearlstein, R. A. New insights about hERG blockade obtained from protein modeling, potential energy mapping, and docking studies. *Bioorg. Med. Chem.* **2006,** *14*, 3160-3173.
45. Aronov, A. M. Predictive in silico modeling for hERG channel blockers. *Drug Discov. Today* **2005,** *10*, 149-155.
46. Jiang, Y.; Lee, A.; Chen, J.; Ruta, V.; Cadene, M.; Chait, B. T.; MacKinnon, R. X-ray structure of a voltage-dependent K^+ channel. *Nature* **2003,** *423*, 33-41.
47. Abraham, J. M.; Saliba, W. I.; Vekstein, C.; Lawrence, D.; Bhargava, M.; Bassiouny, M.; Janiszewski, D.; Lindsay, B.; Militello, M.; Nissen, S. E.; Poe, S.; Tanaka-Esposito, C.; Wolski, K.; Wilkoff, B. L. Safety of oral dofetilide loading for rhythm control of atrial arrhythmias. *J. Am. Coll. Cardiol.* **2014**, *63*, A435.

48. Ficker, E.; Jarolimek, W.; Kiehn, J.; Baumann, A.; Brown, A. M. Molecular determinants of dofetilide block of hERG K^+ channels. *Circ. Res.* **1998**, *82*, 386-395.
49. Guo, D.; Mulder-Krieger, T.; IJzerman, A. P.; Heitman, L. H. Functional efficacy of adenosine A_{2A} receptor agonists is positively correlated to their receptor residence time. *Br. J. Pharmacol.* **2012,** *166*, 1846-1859.
50. Xie, Y.; Yu, M.; Zhang, Y. Iron (II) chloride catalyzed alkylation of propargyl ethers: Direct functionalization of an sp3 CH bond adjacent to oxygen. *Synthesis* **2011,** *2011*, 2803-2809.
51. Yu, Z.; Klaasse, E.; Heitman, L. H.; IJzerman, A. P. Allosteric modulators of the hERG K^+ channel: Radioligand binding assays reveal allosteric characteristics of dofetilide analogs. *Toxicol. Appl. Pharmacol.* **2014,** *274*, 78-86.